

NISTIR 5619

***SPREAD* - A MODEL OF FLAME SPREAD ON
VERTICAL SURFACES**

Henri E. Mitler and Kenneth D. Steckler

February 1993
Issued April 1995
Building and Fire Research Laboratory
National Institute of Standards and Technology
Gaithersburg, MD 20899



U.S. Department of Commerce
Ronald H. Brown, *Secretary*
Technology Administration
Mary L. Good, *Under Secretary for Technology*
National Institute of Standards and Technology
Arati Prabhakar, *Director*

CONTENTS

LIST OF FIGURES	iv
ABSTRACT	1
1. INTRODUCTION	1
2. DESCRIPTION OF THE PROGRAM	2
3. UPWARD SPREAD	2
4. LATERAL SPREAD	4
5. PYROLYSIS	5
6. REGRESSION AND BURNTHROUGH	7
7. FLAME FLUXES	8
7.1 Convective flux	9
7.1.1 Pyrolysis region	9
7.1.2 Preheating region	10
7.2 Flame temperatures	12
7.3 Radiative Flux	13
7.3.1 From burners	13
7.3.2 Flame radiation from burning walls	14
7.4 Flux from the combined flame	16
7.5 Flame heights and flame splitting	17
8. MODEL EVALUATION	17
9. OBTAINING THE INPUT DATA	19
10. USERS' GUIDE	20
11. SUMMARY	23
12. ACKNOWLEDGEMENT	23
REFERENCES	24
NOMENCLATURE	27
FIGURES	30
Appendix A. Sample list of input for PMMA	45
Appendix B. List of subroutines and function subprograms	47
Appendix C: Structure of SPREAD, via block/flow diagrams	54

LIST OF FIGURES

- Figure 1. Side view of a cross-section of the wall, subdivided into its constituent slices. The cross-hatched area is the pyrolyzing region (at time t).
- Figure 1a. Schematic of wall and wall flame. The igniter, a slot burner, is marked B. The igniter fuel and pyrolysis vapors mingle and result in a single "merged" flame. For simplicity, we have assumed that $Z_B = Z_S = Z_{PB}$. The shaded part of the slab is the pyrolyzing zone.
- Figure 2. Idealized pyrolyzing area in a two-zone room-fire simulation.
- Figure 3. The mass-loss-rate data for PMMA, as obtained from the cone calorimeter, is given for several irradiation fluxes by the data points. See text for a description of the solid curves.
- Figure 4. Measured (total, steady-state) fluxes from wall flames back to the wall. The envelope contains much of the available data. The dashed curve is the flux, calculated according to the formulation in this article, at $t = 0$ for a 4 kW slot burner. The abscissa is normalized by the flame heights.
- Figure 5. Schematic of the radiation flux from a burning-wall flame back to the wall, according to Eq.(50).
- Figure 6. The time dependence of the heat of gasification, $h_g(t)$, of untreated Douglas fir plywood, irradiated at 35 and 65 kW/m². The measurements were made in the Cone Calorimeter.
- Figure 7. The heat of gasification of untreated Douglas fir plywood irradiated with 35 kW/m², as a function of the remaining mass.
- Figure 8. The heat of gasification of untreated Douglas fir plywood irradiated with 65 kW/m², as a function of the remaining mass.
- Figure 9. The heat of gasification of untreated Douglas fir plywood irradiated with 85 kW/m², as a function of the remaining mass.
- Figure 10. Position of the upper pyrolysis front as a function of time, for thermally-thick PMMA. Open circles are FMRC data; solid curves are calculated positions for several assumed burner strengths. Burner width is 0.4 m, so that \dot{Q}_b must be multiplied by 2.5 to get \dot{Q}' .
- Figure 11. Position of the upper pyrolysis front as a function of time, for thermally-thick PMMA; NIST experiment. The difference between peak and average values arises because the pyrolysis front is not horizontal (three-dimensional burning). The solid curve is calculated.
- Figure 12. Input data for the particle board calculation.
- Figure 13. Position of the upper pyrolysis front as a function of time, for particle board. Same remarks as for Fig.11.
- Figure 14. χ_A , χ_C , and χ_R , correlated against the smoke-point height. (Note: $\chi_C \equiv \chi_A - \chi_R$).

SPREAD - A MODEL OF FLAME SPREAD ON VERTICAL SURFACES

H.E. Mitler and K.D. Steckler

Building and Fire Research Laboratory

February, 1993

ABSTRACT

This report describes the computer program SPREAD. SPREAD is the explicit implementation of a model which has been developed for predicting the ignition of, and the subsequent rate and extent of fire spread on flat walls in a room using the fire properties of the materials involved. It uses input data from bench-scale tests including the LIFT and the Cone Calorimeter. The principal mode of spread is upward, but the calculations also include the slow lateral spread on the wall. For the latter calculations, the fact that the room produces a two-layer environment has been taken into account (the lateral spread rate within the upper layer is greater than in the lower one). Embedded in the overall model is a general pyrolysis submodel, specially developed for this purpose, which treats arbitrary materials (ablating, char-forming, composite, etc.). SPREAD also calculates the regression of the pyrolyzing surface, including the possible burnout of the wall/slab at any point. The program has been compared to experimental data for wood particle board and for PMMA. The structure of the program is given in a set of appendices.

Key words: computer models; fire growth; fire models; fire spread; mathematical models; upward spread; wall fires

1. INTRODUCTION

The objective of this work is to develop a method for predicting the rate and extent of fire spread on wall surfaces in a room, and thence the rate of heat release (RHR), using the fire properties of the wall material.

Modeling wall fires is important for two related reasons: first, wall fires spread upward rapidly on vertical surfaces, which can lead to rapid flashover in rooms. Second, accurate modeling of wall fires will enable us to assess the flammability of wall-covering materials from bench-scale tests of the material, rather than having to rely on much more expensive and time-consuming full-scale tests.

The program and what it does is briefly described in Section 2. Lateral and upward spread are discussed in Sections 3 and 4; pyrolysis and burnthrough in Sections 5 and 6; flame fluxes in Section 7, experimental comparisons in Section 8, and how to obtain the needed data in Section 9. Detailed information about the program itself is given in the Appendices.

2. DESCRIPTION OF THE PROGRAM

For a given ignition source, and given the appropriate thermophysical parameters of the wall material, SPREAD calculates the time to ignition of the wall, the location and extent of the initial pyrolyzing area, the mass-loss rate, the rates of upward and lateral spread of the fire, and the resulting rate of heat release.

The input includes the experimental rate of heat release from the Cone Calorimeter; this rate is proportional to the mass-loss rate. Thus, the calculation **automatically** takes charring and transient pyrolysis into account, at least to a first approximation. The input also includes the external flux impinging on the wall as a function of time and position, which the program then takes into account in making the above calculations. Currently, the program allows for just two external fluxes: the mean external flux impinging on the part of the wall contiguous to the upper layer, and that contiguous to the lower layer. Generalization to more than two fluxes should be quite straightforward. The first part of the input data required (geometry, thermophysical parameters) is given in Appendix A. For the lateral-spread calculation, the program takes into account the fact that the upper part of the wall has a different temperature than the lower part, so that the lateral-spread rate is greater in the upper region. Thus, the effect of having two layers is explicitly taken into account (see Section 4). Note that different heating fluxes impinging on the upper and lower walls influences the lateral spread rate only indirectly, through the resulting wall surface temperature.

The power output of the ignition source is user-specified, and can be an (almost) arbitrary function of time. Among the things the program does not yet have in it are the effects the presence of the ceiling has on the burning and spread rates (except insofar as the ceiling traps the upper gas layer). It also does not include the effect of self-extinguishment.

It is important to note that the fire spread process is a result of closely coupled gas-phase and solid-phase phenomena. For example, the wall (solid phase) surface temperature above the pyrolysis zone depends on the heat flux from the flame and heated plume (gas phase) which, in turn, depends on the surface temperature of the wall. Similarly, the mass-loss rate from the pyrolyzing part of the wall depends on the heat flux from flame, which depends on the mass-loss rate of the wall. Consequently, the equations describing these phenomena must be solved simultaneously. The program does this by the method of successive substitutions, using a preset number of iterations.

This report also includes

- a. a list of needed input (Appendix A and Section 9),
- b. flow diagrams for the program (Appendices B and C),
- c. a nomenclature table,
- d. some comparisons with experimental data (see Section 8), and
- e. a users' guide (Section 10).

The assumptions made and the limitations of the calculations are indicated throughout the report. In reference to item b, the source of the information which is not usually found in the literature is given in Section 9.

3. UPWARD SPREAD

"The upward spread rate" of a wall fire means the upward velocity of the upper **pyrolysis front**. Generally, it is assumed that the fire is two-dimensional (i.e., independent of horizontal position on the

wall). When that symmetry is missing, the definition must be generalized to the mean position of the front.

It would be very useful to have an explicit expression for the upward spread rate. The dynamics of the process is conceptually simple: convective and radiative fluxes from the flame heat the solid ahead of ("above," for upward spread) the pyrolysis front, causing the solid to reach its pyrolysis temperature; when the pyrolysis rate becomes sufficiently high that the local fuel vapor concentration attains the lower flammability limit, that section of the wall may be said to have attained its "ignition temperature," and the pyrolysis front will have spread to that region.

Several researchers have attempted to generalize the results of de Ris, described in Section 4, to the upward spread process, with some success. In fact, a number of analytic formulations of the upward spread process have been developed (see Cleary 1991, Kulkarni 1991, Kulkarni 1992, Magnusson 1985, Mitler 1986, Quintiere *et al* 1986, Saito *et al* 1985, and Wickström 1987).

The approach used here is different. It is possible, in principle, to follow one of the analytic approaches mentioned above, in developing an algorithm to calculate the upward spread rate. They are, however, somewhat complicated; more important, they generally depend on one or more unrealistic simplifying assumptions (such as uniformity of oxygen concentration and gas temperature, constancy and uniformity of any externally imposed fluxes, etc.). In order to avoid these, the movement of the pyrolysis front is not calculated analytically, in this algorithm; instead, the front is assumed to move up to any point along the surface as it heats up to a critical temperature T_c ; we will assume that an ignition temperature T_{ig} exists, and that $T_c = T_{ig}$. Flammability limits are ignored: it is implicitly assumed that pyrolysis will be sufficiently great that this limit is immediately exceeded. The temperature is calculated at a certain number of (fixed) points, or nodes. Unlike the case for most of the analytic treatments, the fluxes leading to the heating of the wall may be time-varying as well as nonuniform with respect to vertical position on the wall; the external conditions can also vary both with time and along the surface. We choose $N+1$ equally-spaced nodes; the value of N is internally calculated so that ignition will first occur at a node (see Fig.1). The approach adopted here is thus less elegant but more general, straightforward, and powerful; the principal assumptions made are that there exists a well-defined ignition temperature T_{ig} , that there is no lateral diffusion of heat (even though the slab is being heated at different rates at different heights), that the material does not melt, and that it has a well-defined heat of vaporization. It is also assumed that heat diffuses inward, through the slab, by conduction only (that is, that there is no internal radiative heat transfer), and that the geometry is such that the problem is one-dimensional. Figure 1a shows a few more of the relevant dimensions, and is included here for the sake of clarity.

Since the flame extends above the pyrolysis zone, the section of wall above it is heated. If and when the surface temperature reaches T_{ig} at a node, the pyrolysis front is taken to have arrived there. While the front lies between two nodes, it advances upward at a rate which we approximate as follows: We assume that the pyrolysis front has progressed toward node m (at z_m) from its position at the previous time step, $z_p(t_s)$, in proportion to the degree to which the temperature at that node, T_m , has progressed toward T_{ig} . Thus,

$$z_p(t_{s+1}) = z_p(t_s) + [z_m - z_p(t_s)](T_m^{s+1} - T_m^s)/(T_{ig} - T_m^s) \quad (1)$$

where T_j^k is the temperature at node j , at time t_k . Note that the highest pyrolyzing node is $m - 1$. The lowest pyrolyzing node is ℓ . We return to the details of the upward-spread problem in Section 5. First, we consider how to calculate lateral spread, to complement the upward spread.

4. LATERAL SPREAD

A fire ignited on a section of a wall will spread upward, laterally, and (to a small extent) downward. Generally, the spread rates increase with time. We now consider lateral spread.

A theoretical expression for the lateral spread rate V_s of a flame along the surface of a thermally-thick solid was first developed for a laminar flame on a horizontal surface by de Ris (1969). This expression for the spread velocity was found to be valid for turbulent flames as well (Quintiere, 1981). The velocity can be expressed in terms of the experimentally-determined parameters Φ and $k\rho c$ (of the material):

$$V_s = \Phi/[k\rho c(T_{ig} - T_s)^2]; \quad (2)$$

V_s is the rate of spread over a surface when the entire slab is initially at the temperature $T = T_s$, and T_{ig} is the ignition temperature of the material. There is a different expression for the thermally thin case. However, thin materials are generally laminated onto a thicker backing, so that the ensemble is thermally thick. That is the way the samples are tested in bench-scale tests. The expression (2) for spread in opposed flow has been found to be equally valid for lateral spread on vertical surfaces. The LIFT apparatus has been used to obtain Φ , $k\rho c$, and T_{ig} experimentally.

More generally, it has been noted that sometimes an external heating flux ϕ is needed in order to get spread: i.e., there will be no spread unless the flux ϕ exceeds the critical flux, ϕ_c . Note that if there were no flame, the critical flux would eventually bring the wall surface temperature up to a steady-state temperature T_c . If the actual wall temperature is less than T_c , it might correspond to a larger flux operating for a short time; on the other hand, if the wall temperature is greater than T_c , the external flux **must** be greater than ϕ_c . Thus if $T_s < T_c$, the external flux might be $> \phi_c$, but if $T_s > T_c$, we are guaranteed that $\phi > \phi_c$. Therefore a reasonable approximation to the generalization is to replace Eq. (2) with

$$V_s = \begin{cases} Eq(2) & T_s \geq T_c \\ 0 & T_s < T_c \end{cases} \quad (3)$$

The pyrolysis area is taken to be a (growing) rectangle, whenever the ambient conditions are uniform. T_s is taken to be the instantaneous wall temperature in the region adjacent to the pyrolyzing region (not the space above the pyrolysis zone). Thus for $T_s \geq T_c$, the pyrolyzing region is a rectangle of width $w(t) > w(0) \equiv w_o$, and

$$w(t) = w_o + 2 \int_0^t V_s(\tau) d\tau \quad (4)$$

The pyrolyzing zone will cease to be a simple rectangle when part of it lies in the upper layer, since the lateral spread will be faster there (see Fig.2). But then the wall fire is no longer two-dimensional, and it no longer has a single well-defined width. Yet that is needed to get the power output per unit width (needed, in turn, to obtain the flame height). We thus need to find an appropriate mean width. A plausible approximation is obtained by using an equivalent-area rectangle as the model zone: First, we note that the mass-loss rate per unit area varies with height, in general; hence

$$\dot{m}(t) = w_d \int_{z_b}^{z_M} \dot{m}''(z) dz + w_u \int_{z_M}^{z_p} \dot{m}''(z) dz \quad (5)$$

where w_d and w_u are the pyrolysis zone widths in the lower and upper layers, respectively. Then

$$\dot{Q}(t) = \chi_A \Delta H_c \dot{m}(t) \quad (6)$$

(it is assumed that χ_A is constant and the same in the two layers). Thus, we shall use

$$\dot{Q}' \equiv \dot{Q} / \bar{w} \quad (7)$$

where

$$\bar{w} = \begin{cases} w_d & z_M \geq z_p \\ \frac{w_d(z_M - z_b) + w_u(z_p - z_M)}{z_p - z_b} & z_p > z_M > z_b \\ w_u & z_M \leq z_b \end{cases} \quad (8)$$

This approximation is readily seen to be correct in the limits where the entire pyrolyzing zone lies in the hot upper layer ($z_M < z_b$) and where it lies entirely in the lower layer ($z_M > z_p$). Still better would be to use a mass-loss-weighted mean value, rather than an area-weighted mean, but that makes for more complicated expressions. Moreover, we note that the lateral spread rate is usually two orders of magnitude slower than the upward spread rate, so that it can become important (relatively speaking) only after the upward pyrolysis has ceased.

5. PYROLYSIS

In order to predict the upward spread rate, we must know the fluxes from the flame; this in turn requires that we know the flame length (height). To know the flame length requires that we know the total power output; finally, that requires that we know the heat of combustion and the mass-loss rate. Thus we first need to predict the mass-loss rate of a fire ignited on a vertical surface, given the dimensions of the pyrolyzing zone, some material parameters corresponding to the wall, any external heat fluxes, and some properties of the flame and plume.

The burning process consists of closely coupled gas-phase and solid-phase phenomena. The solid-phase processes are transport of heat through the solid (usually by conduction), the pyrolysis of the material, and the transport of the gaseous fuel to the surface. The gas-phase phenomena include combustion and fluid flow. The two phases are coupled through the emergence of the fuel into the gas, and the convective and radiative feedback from the hot gases back to the surface of the solid.

We need the pyrolysis rate of a burning vertical slab which is exposed to specified external fluxes (as well as to the heating flux from its own flame). These external fluxes must either be supplied by the user, calculated by a room-fire model and then passed to the program, or produced by some combination of the two.

The burning rate in the original SPREAD program was calculated in one of two ways, at the user's option: first, an energy balance is made at the surface. This is a steady-state integral model, and applies, in principle, only to materials that do not melt, char, or burn through, and which have a well-defined

ignition temperature. PMMA approximately satisfies these conditions, and is the prototype material. This procedure has been described by Mitler (1988), and the successful results of its use given in Steckler and Mitler (1988). This option has, however, been removed from the current version, since the program is to be used within CFAST, and it was considered preferable not to force the user to make such a choice in that program. The choice has been temporarily removed by bypassing those sections of the code (though not removing them, since we may decide to reinstate that calculation at some future date). See Appendix C, section C4 (p.39) and C8 (pp.45 and 46).

The second method for calculating the burning rate uses experimental values of \dot{m}'' from the Cone Calorimeter. This is described in Mitler (1990). Eqs.(22)-(25) in that article give the mass-loss rate based on cone-calorimeter output:

$$\dot{m}''(t) = \xi(t) \dot{m}_c''(\tau) \quad (9)$$

where \dot{m}_c'' is the cone (experimental) mass-loss rate at the scaled time τ ,

$$\tau \equiv \int_0^t \xi(t') dt' \quad (10)$$

$\xi(t)$ is the "acceleration" of the pyrolysis rate due to the net heating flux impinging on the material being greater (smaller) than that to which the sample is exposed during the cone test. For an ablating material,

$$\xi(t, \tau) \equiv \phi_{\text{net}}(t) / \phi_{\text{net},c}(\tau) \quad (11)$$

where the denominator is given by

$$\phi_{\text{net},c}(\tau) = \alpha_w \phi_{\text{ex},c} + \phi_{f,c}(\tau) - \phi_{\text{rr}}(\tau); \quad (12)$$

and the subscript c stands for Cone. ϕ_{ex} is the external flux from the cone's heater coils, ϕ_f is the flame heating flux, and ϕ_{rr} is the reradiation flux. How these fluxes are obtained is discussed in Section 7. The cone flux is very nearly constant, so that the dependence on τ in Eq.(11) is very weak, and we will hereafter just write $\xi(t)$.

Use of Eqs.(9)-(12) implicitly assumes that the heat of gasification, defined as

$$h_g(t) \equiv \phi_{\text{net},c}(t) / \dot{m}_c''(t) \quad (13)$$

where the subscripts "c" refer to measurements made in the Cone Calorimeter, is a unique "signature" for each material, and is independent of the radiation flux used.

Note that Eqs.(9)-(13) also implicitly assume instantaneous transport of the pyrolysis gases to the surface; for charring pyrolysis, in fact, it actually takes a time of the order of

$$t_x \approx x^2 / 4\alpha \quad (14)$$

for the flux "signal" to reach the depth x , assuming no radiative heat transfer. Since a time delay is already "built in" for the mass loss rate in the Cone, however, and, moreover, t_x is approximately

independent of the impinging flux (according to Eq(14)), Eqs.(9)-(11) can be expected to give a reasonable approximation to the correct answer.

It is appropriate to ask whether Eq.(9), though plausible, is valid. In Fig.3, the mass-loss-rate data for PMMA, as obtained from the cone calorimeter, (Babrauskas, 1984) is given for several irradiation fluxes by the data points shown. The data from the 50 kW/m² run was fitted by a curve, and was then used to "predict" what the mass-loss-rates would be at irradiation levels of 25 and 75 kW/m², using Eqs.(9)-(12). The results are shown in Fig.3. It is seen that the equations yield fits to the other two sets of data which can be qualitatively described as "good" (no correlation coefficient or other fitting parameter has been used to give a quantitative evaluation).

6. REGRESSION AND BURNTHROUGH

Once ignition has occurred at a node, the surface must regress, as the material behind it loses mass. As soon as the pyrolysis front reaches a new node (say, z_n), the program ceases calculating the temperature distribution (in depth) at that point; instead, the assumption is made that the surface temperature remains T_{ig}, and the program proceeds to calculate the regression rate at that point. This section describes how that is done.

SPREAD currently calculates the mass-loss rate at each pyrolyzing node, using the flux at that height from the flame, plus one (mean) external, user-given, flux (or one supplied by a room-fire model into which SPREAD is embedded). The program then calculates $\dot{m}_i''(t)$, and returns the mean mass-loss rate, $\bar{m}''(t)$. The lower regions of the wall will have been pyrolyzing for a longer time than the upper regions; they will therefore be pyrolyzing at a rate consistent with later parts of the experimental mass-loss curve, and therefore at a different (usually higher) rate than the upper regions. Since they will have been regressing a longer time than the upper regions as well, they will generally burn through earlier.

We now examine how the mass-loss rate and regression are calculated at each node. As described above, the pyrolysis rate $\dot{m}_i''(t)$ is calculated at each node i from experimental values of the mass-loss rate (usually, from the Cone Calorimeter). Given $\dot{m}''(t)_{\text{cone}}$, the transformation (9) will give a different $\dot{m}_i''(t)_{\text{real}}$ at each pyrolyzing node i, because the (net) flux history at each node will generally be different from that at every other node. Pyrolysis takes place at nodes ℓ to m-1.

Suppose that at time t_{s+1}, node m is found to be (newly) involved. As soon as this new node is involved, the surface begins to regress at that (new) point. Now, the interval **during which** the new node (m) has been reached and passed is

$$\Delta t_{s+1} \equiv t_{s+1} - t_s.$$

However, the time during which the surface at node m has actually regressed is not Δt_{s+1} , but the fractional time period

$$\delta t_{s+1} = \left[\frac{z_p^{s+1} - z_m}{z_p^{s+1} - z_p^s} \right] \Delta t_{s+1} \quad (15)$$

Since we have simply interpolated linearly, this is merely an approximation.

Then the mass-loss rate at node m is given by Eq.(9), and it starts to lose mass at the ignition time

$$t_{ign,m} \equiv t_{s+1} - \delta t_{s+1}. \quad (16)$$

In principle, this small delay should be taken into account. In this version of the program, however, this correction has not yet been introduced; that is, the program "assumes" that ignition occurs at t_{s+1} ; this is a negligible error. Thereafter, the regression at that node takes place over **full** time periods.

Eqs.(9) to (12) then apply at node m: Eq.(9) becomes

$$\dot{m}_m''(t) = \xi_m(t) \dot{m}_{cone}''(\tau_m) \quad (17)$$

However, Eq.(10) must be replaced by

$$\tau_m \equiv \int_{t_m}^t \xi_m(t') dt' \quad (18)$$

where t_m is the moment at which mass loss began at node m (about the same as the ignition time there), and

$$\xi_m(t) = \phi_{net,m}(t)/\phi_{net,cone}(t) \quad (19)$$

For subsequent node ignitions, the starting times will be appropriately later. The times τ_k ($k = m, m+1, \dots$) must be saved during the calculations.

Having found the mass-loss rate per unit area at each node i, we then have the distance through which the surface regresses at the ith node, in the time interval Δt_s :

$$\Delta \theta_i^s = \frac{1}{\rho} \int_{t_{s-1}}^{t_s} \dot{m}_i''(z_i, t) dt = \frac{\dot{m}_i''}{\rho} \Delta t_s \quad (20)$$

Thus

$$\Theta_i(t_{s+1}) \equiv \Theta_i^{s+1} = \Theta_i^s - \Delta \theta_i^s \quad (21)$$

Note, however, that a material may have variable density. This is the case, for example, with particle board. In order to avoid the need of specifying $\rho(x)$ in Eq.(20), it is simpler to use $m''(0)$ as the "mass thickness"; that is, we need consider only $\Delta m''$, rather than $\Delta \theta = \Delta m''/\rho$.

$\Delta m''$ is given by the integral in Eq(20), **without** the $1/\rho$ factor. Thus, burnthrough occurs when

$$\Sigma \Delta m'' \geq m''(0) \quad \text{implies burnthrough} \quad (22)$$

where the sum is over the time steps taken (i.e., it is the cumulative mass loss at that node).

7. FLAME FLUXES

In order to determine the temperature history of the wall surface prior to ignition, $T_s(z,t)$, it is necessary to know the heating flux to the wall from the flame, $\phi_w(z,t)$. It is equally needed in the pyrolyzing region, to determine the mass-loss rate. The simplest analyses assume(d) that ϕ_w is constant between the

pyrolysis front and the flame-tip height, and zero above (Orloff *et al* (1975), Saito *et al* (1985), etc.). This will give rise to a "leap-frog" growth rate (i.e., one discontinuous in the first derivative). On the other hand, Sibulkin and Kim (1977) assumed, for their laminar-flame experiments, an exponentially decaying flux; this is more appropriate, and gave results in fair agreement with their experiments. There is now enough information available that a realistic calculation of the heating fluxes from turbulent fires can be made without the need to posit one; this permits calculations of upward spread rates from first principles.

Quintiere (1988) has collected much of the available data, and displayed it in Fig.6 of that article; part of that figure is reproduced here in Figure 4. Examination of that figure (which looks rather like a map of Florida) suggests that the total heating flux is approximately constant in the pyrolyzing region (and perhaps beyond), and falls as a power law starting at x_v , somewhere in the heating region:

$$\phi_w(x) \approx \phi_v [x/x_v]^{-n} \quad (23)$$

where ϕ_v is (evidently) the value of the wall flux at x_v . An "eyeball" fit of the curve yields $n \approx 2.3$. The figure also suggests that this behavior -- that is, a nearly constant flux of 20 to 30 kW/m² up to about 40% of the flame-tip height, etc. -- is (nearly) universal; however, there apparently is considerable scatter of the data. Moreover, all these data pertain to gas-burner flames of moderate (20 to 80 cm) size. That "scatter" is here interpreted to mean that ϕ_v does not, in fact, have a unique value.

There are two main problems associated with this approach (i.e., taking ϕ_w to be a constant up to some height x_v , followed by the use of Eq.(23)): first, careful measurements have shown that the radiation flux on the pyrolyzing section of the slab is in fact not constant, but rises (more or less linearly) with height (Orloff *et al* 1977; this is also found in the results of Markstein (1990)). On the other hand, the convective flux in this region falls with height more slowly than the radiation flux rises, so that the total wall flux will rise. The second problem is that neither x_v nor ϕ_v are known. There are other problems as well, but they are less important.

With regard to the first problem, note that the results shown in Fig.4 are not inconsistent with a rising flux (within limits) in the lower section of the wall. Indeed, instead of taking $\phi_w = \text{const.}$ in the region $z \leq z_p$, the fluxes ϕ_r and ϕ_c in the pyrolyzing region can be estimated (Mitler (1988)); however, it is not shown there how to find the flux in the heating (over-pyrolysis) region. We therefore seek expressions for $\phi_r(z)$ and $\phi_c(z)$ in this region, as well (see Section 7.1.2).

The heating flux from the flame/plume to the wall is the sum of convective and radiative fluxes. We will now find expressions for each of these fluxes.

7.1 Convective flux

7.1.1 Pyrolysis region

The convective flux is calculated in two ways: first, in the pyrolysis region, the convective flux is given by the expression used in Mitler (1988) and de Ris (1979) (derived from Spalding's (1953) formulation):

$$\phi_c = \frac{\dot{m}'' B' H_v}{\exp(\dot{m}'' c_p / h) - 1} \quad (24)$$

where h is the heat transfer coefficient, c_p the specific heat of the gas, and B' is the Spalding mass-transfer potential B , corrected for losses. The second is discussed in Section 7.1.2. The Spalding (mass transfer) number, before correction for losses, is defined as

$$B \equiv [\nu y_o H_c + c_p(T_g - T_s)]/H_v \quad (25)$$

where ν is the stoichiometric fuel/air mass ratio, y_o is the mass fraction of oxygen in the air, H_c is the (lower) heat of combustion, c_p the specific heat of air, T_g the ambient gas (air) temperature, T_s the temperature of the pyrolyzing (or evaporating) surface, and H_v the gross heat of vaporization. In order to take the incompleteness of combustion and the losses via radiation into account, B must be replaced by B' , defined just as above, but with H_c replaced by

$$H_c' = (\chi_A - \chi_R)H_c \quad (26)$$

where χ_A is the efficiency (completeness) of combustion and χ_R is the fraction of the (theoretical) heat release rate which is lost from the combustion region by radiation.

As for the factors in the exponential in Eq.(24), experiment shows that h/c_p is 12 ± 2 g/m²s. Tewarson, Lee, and Pion (1980) have measured it to be 12.7 and 13.6 g/m²s, for small samples in their apparatus. For the vertical orientation, Mitler (1988) found that 11.8 was the value most nearly consistent with other data. We note that in order to find ϕ_c , we must have dm''/dt , which is what we are trying to solve for in the first place! Thus the equations are strongly coupled, and must be solved simultaneously. This is done by solving the equations iteratively (by successive substitutions), as described earlier.

7.1.2 Preheating (over-pyrolysis) region

Next, consider the heating, or over-pyrolysis, region; there is no mass loss there, and we cannot use the above procedure. Instead, we note that the convective flux to the wall is

$$\phi_c(z,t) = h(z)[T_p(z,t) - T_s(z,t)] \quad (27)$$

where T_p is the plume temperature at z and T_s the surface temperature there; we take $T_p(z,t) = T_f(z,t)$ up to the flame tip height (the height as defined by Steward (1970); that is, the place where the flame intermittency is 50%).

Between the pyrolysis front and the flame tip, the wall temperature decreases with height. The mean gas temperature also falls with height, in the intermittent-flame region. It is important to note that Eq.(27) is in fact valid in the pyrolysis region, as well, but with h modified somewhat, as discussed below. We shall discuss h , T_f , and T_s in turn.

We can infer effective values of $h(x)$ from the data obtained by Orloff *et al* (1977) upon burning a 12-foot-high slab of PMMA, in the (quasi) steady state. They showed that the burning rate was

$$\dot{m}''(x) = 5.3241 + 3.966x \text{ g/m}^2\text{s} \quad 0 < x < x_p \quad (28)$$

We can also infer from their results that the radiation flux was, as a function of height,

$$\phi_{rf} = 11.0 + 7.483 x - 0.1 x^2 \text{ kW/m}^2, \quad 0.5 \leq x \leq 3.56 \quad (29)$$

We can use these steady-state results for the transient case, because the spread rates are quite slow in comparison with the fluid-flow velocities. Incidentally, we note from Eq.(28) that, at least for this large wall fire, the total heating flux to the wall was indeed not uniform in the pyrolysis region (c.f. first paragraph in Section 7).

The fact that there is substantial mass loss at the bottom of the slab implies a substantial total heating flux there. On a number of grounds, we should take the radiation flux at the bottom of the pyrolysis/flame zone to be nearly vanishing (rather than 11 kW/m²). The conclusion is that the convective flux there is larger than the 5.5 kW/m² estimated by Orloff et al. They assumed that the convective flux to the surface is constant. If, instead, we take the radiation flux to rise more or less linearly from zero at the base of the fire, as Markstein found, ϕ_c must be a decreasing function of height, rather than a constant.

We note that Eq.(27) holds in the pyrolyzing region as well as in the heating region. However, the heat transfer coefficient in the pyrolysis region should be replaced by h_{wb} (the subscript "wb" stands for "with blowing"). We now indicate how this was obtained: It is easy to show (see, for example, Marxman (1965)) that blowing from the wall reduces the heat transfer to the wall by the factor $\ln(1+B_c)/B_c$, where B_c is the convective Spalding number, related to B' via

$$B_c \equiv B' / (\phi_c / \dot{m}'' H_v). \quad (30)$$

When there is heat transfer by convection only -- that is, no radiation (or reradiation) -- B_c reduces to B' . Thus the convective flux in the pyrolysis zone is given by

$$\phi_c = [\ln(1+B_c)/B_c] \phi_{co}, \quad (31)$$

where ϕ_{co} is the convective flux **without** blowing. Eq.(30) allows one to write \dot{m}'' in the form first used by Spalding:

$$\dot{m}'' = (h/c_p) \ln(1 + B_c). \quad (32)$$

If we define the heat transfer coefficient **with blowing** by

$$h_{wb} = h[\ln(1+B_c)/B_c] \quad (33)$$

then we can write Eq.(32) in the form

$$\dot{m}'' = B_c h_{wb} / c_p. \quad (34)$$

The variation of \dot{m}''/dt with height on the wall thus depends on the variation of h and of B_c , with height. From Eq.(34) and from the above data on \dot{m}'' and h_{wb} , we find that $B_c(0)=0.329$ and $B_c(3.56)=3.253$. Further analysis of these data and of associated measurements made by Orloff et al then shows that

$$h(x) \approx 18.0 + 7.1 e^{-px} \text{ W/m}^2\text{C} \quad (35)$$

This asymptotic value -- 18 W/m²C -- is close to the value inferred in Mitler (1988): $h = (h/c_p)c_p = (11.83)1.34 = 15.9$, or that inferred from Tewarson et al (1988): $h = (12.7 \text{ to } 13.6)c_p = 17.0 \text{ to } 18.2$. The value of p is readily found by making a calculation of $h(x)$ at some intermediate height, as indicated above Eq.(28). That yields the value

$$p \approx 8.57 \chi_R$$

7.2 Flame temperatures

According to Eq.(27) we must also know how T_f varies with x . Gas-phase behavior - combustion and fluid dynamics - is relatively independent of whether the fuel issues from a burner or from a pyrolyzing surface. Therefore we expect $h(x)$ to be about the same in the two cases. Ahmad and Faeth (1979) give experimental values of $\phi_c(x)$ for $x > x_p$, from which one can infer these temperatures:

$$T_f(x) \approx 351.6 + \phi_{\text{exp}}(x)/h(x) \quad (36)$$

where $\phi_{\text{exp}}(x)$ are the experimentally-established values of $\phi_c(x)$, and $h(x)$ is given by Eq.(35). Inserting those, one finds

$$T_f(x) = 298 + 1113 \exp[-\alpha(x/x_p)^2], \quad (37)$$

with

$$\alpha = 0.023 \pm .002$$

The expression is not very useful in this form, however: x should be normalized by x_f , the flame height, rather than by x_p . Moreover, the peak temperature must depend on the adiabatic flame temperature and on the fraction of energy lost, especially by radiation. To a first approximation, however, we shall assume that all flames are very similar; we can then relate x_p to x_f as follows:

There is a well-known correlation of wall-flame height with power output per unit width (Hasemi 1986):

$$x_f = \beta (\dot{Q}')^{2/3} \quad \text{m} \quad (38)$$

(with \dot{Q}' in kW); see figure 1a for the significance of x_f . Hasemi uses $\beta = 0.06$. Other authors have used different values for β ; for example, Ahmad and Faeth use 0.050, while Steckler (personal communication) finds 0.052 to be a good value. If we use Eq.(38) to give x_f , with $\beta = 0.052$, we find that $x_f/x_p = 4.02$, which is consistent with Ahmad and Faeth's experimental findings.

On the other hand, Markstein (1990) found that better results are obtained with the correlation

$$x_f = \beta_2 (\dot{Q}')^{1/2} \quad \text{m} \quad (39)$$

where $\beta_2 \approx 0.14$. We have found better results using Eq.(39), as well (see Mitler, 1990), and it is therefore used in the program, rather than (38). When we use (39) instead of (38), then $x_f/x_p = 5.26$, which is higher than Ahmad and Faeth's observation. If we use the latter nevertheless, then Eq.(37) can be written as

$$T_f(x) = 298 + 1113 \exp[-0.636(x/x_f)^2]. \quad (40)$$

This is the expression that is used. Finally, we need to have $T_s(x)$ in order to be able to use Eq.(27) to find $\phi_c(x)$. In the algorithm described in this paper, $T_s(x)$ is calculated at each node, at every time step, assuming one-dimensional conduction heat transfer. The explicit scheme used here is essentially the same one as is used in FIRST (Mitler and Rockett 1987), but with the modulus $(\Delta x)^2/\alpha\Delta t$ changed from 2 to π to give greater stability and an exact value for the temperature at the surface after one time step. Evidently one could replace that algorithm with another, such as is used in CFAST. However, we need $\phi_c(x,t)$ in order to find $T_s(x,t)$. This problem is resolved by solving the coupled equations simultaneously, by successive substitutions, as already described in Section 2.

7.3 Radiative Flux

7.3.1 From burners

There is limited information about the dependence of the radiation flux with height. The most thorough and accurate measurements have been made by Markstein (1990). He measured the radiation fluxes from wall flames, where lightly-sooting gaseous fuels were emitted from a number of sintered metal (vertical) burner panels. This arrangement permitted the experimental simulation of wall pyrolysis. The vertical extent of the (combined) panels, x_p , corresponds to the "pyrolysis" height. By altering the number of these panels, the extent of the "pyrolysis" zone could be changed. He found that the peaks of his distributions all lay about 1/3 of the way up to the flame tip; that is, the smoothed fits to the flux distributions all have peaks at $x_{\max} \approx 0.35 x_f$. Although good smooth fits were made to the distributions, there was, at the time of writing, no way given to obtain the parameters and coefficients in the expression *a priori*. Another peculiarity is that he measures a substantial flux at the origin, even though theory indicates that it should be close to vanishing, there.

The measurements are not entirely consistent among themselves, either: Faeth and others (see, for example, Ahmad and Faeth (1978, 1979)) find a power-law fall-off for the tail of the distribution, whereas Kulkarni *et al* (1991, 1992) find an exponential fall-off.

Whatever distribution is chosen for the radiation flux, it must satisfy a simple symmetry condition: since half the flame flux moves away from the wall and half towards the wall,

$$\int_{z_{pb}}^{\infty} \phi_r(z) dz = \chi_R \dot{Q}' / 2 \quad (41)$$

where it has been assumed that no flux falls outside a zone whose width is w , and which is bounded below by z_{pb} , the position of the bottom of the pyrolyzing region (or z_s , the level of a slot burner).

A convenient and reasonably good (within 20%) approximation to Markstein's (1990) experimental burner fluxes is the exponential distribution

$$\phi_{rb}(X) = \begin{cases} FX(1 - BX) & 0 \leq X \leq X_m \\ \frac{1}{2}FX_m \exp[-\lambda(X - X_m)] & X > X_m \end{cases} \quad (42)$$

where

$$X \equiv z - z_s \quad (43)$$

F is, evidently, the initial slope of the distribution. From Eq.(42), the peak (X_m) is found to lie at

$$X_m = 1/2B \quad (44)$$

As discussed above, experiment shows the peak to lie at $X_m \approx X_f / 3$. It follows that

$$B = 1.5/X_f \quad (45)$$

Moreover, noting that the radiation flux at the flame tip (the 50% intermittency point) is about 25% of what it is at the peak, we must have

$$\lambda = 1.5 (\ln 4)/X_f = 2.079/X_f. \quad (46)$$

Finally, Eq.(41) yields

$$F = \frac{13.5 \chi_R \dot{Q}'_b}{(1 + 3/\ln 4) X_f^2} \quad (47)$$

where \dot{Q}'_b is the burner power output per unit width. Use of Eq.(38) with $\beta = 0.052$ yields

$$F = 1578 \chi_R (\dot{Q}'_b)^{-1/3} \text{ kW/m}^3, \quad (48)$$

with \dot{Q}'_b in kW/m^3 ; while use of Eq.(39) yields

$$F = 217.7 \chi_R \text{ kW/m}^3, \quad (49)$$

instead. Note that it is more satisfying to have the slope F be independent of the power output, based on the physical consideration that the behavior of the flame near the base should be independent of what transpires above. This is one of the reasons for preferring Eq(39) over Eq(38). Actually, Markstein has measured the slope to be $F = 164 \chi_R \text{ kW/m}^3$, which is indeed consistent with the independence of F from \dot{Q}'_b , and is the value used in the program.

7.3.2 Flame radiation from burning walls

It has been observed that for large wall fires, the flux peak lies at or above x_p . For example, Orloff et al (1975, 1977) found the peak at or above the pyrolysis front, which is about 3/4 of the way up to the flame tip, in their experiment. This indicates that we cannot simply use the burner radiation flux expression (42), since the peak, according to Eq(42), lies at $x_{\max} = x_f/3$. In Markstein's experiments, too, it was found that for the largest number of panels, $x_p \approx 0.43x_f$, which is $> x_f/3$.

Although there is a dearth of data on radiation flux from burning walls, there are enough semi-quantitative items of information (de Ris and Markstein, private communications) to permit the construction of a reasonable expression:

$$\phi_I(x) = \begin{cases} \lambda x & 0 \leq x \leq x_u \\ \lambda x_u + (x - x_u) \phi'_o & x_u < x \leq x_p \\ \phi_p \exp[-v(x - x_p)^2] & x_p < x \end{cases} \quad (50)$$

where

$$\lambda = 164 \chi_R \text{ kW/m}^3 \quad (51)$$

(that is, $\lambda = F$) and ϕ_p is given by

$$\phi_p = k x_f, \quad (52)$$

where

$$k = 24734 \chi_R \text{ W/m}^3. \quad (53)$$

The flux produced by Eq(50) is shown schematically in Fig.5. The middle expression in Eq.(50) must be ϕ_p at $x = x_p$. Hence the slope ϕ_o' is given by

$$\phi_o' = (\phi_p - \lambda x_u)/(x_p - x_u). \quad (54)$$

Also,

$$\nu = \ell n4/(x_f - x_p)^2. \quad (55)$$

Finally, x_u is found from the integral (41):

$$x_u = \frac{(\chi_R \dot{Q}'/\chi_A) - \phi_p [x_p + \eta_o (x_f - x_p)]}{\lambda x_p - \phi_p} \quad (56)$$

where

$$\eta_o \equiv \sqrt{(\pi/\ell n4)} \approx 1.50538$$

Under some circumstances, x_u might be calculated to be negative, which would be unphysical. In that case, we can no longer use Eqs(52)-(54) or (56). Instead, we then take

$$x_u = 0, \quad (57)$$

$$\phi_p = \frac{\chi_R \dot{Q}'}{x_p + \eta_o (x_f - x_p)} \quad (58)$$

and

$$\phi_o' = \phi_p/x_p \quad (59)$$

On the other hand, we want to have the flux increasing monotonically up to (at least) x_p . Hence if x_u is such that $\lambda x_u > \phi_p$, we again modify the calculation so that the flux rises to a maximum at x_u' and stays constant thereafter, up to x_p :

$$\text{Define } D \equiv 2x_p + \eta(x_f - x_p); \quad (60)$$

then

$$x_u' = 0.5 [D - \sqrt{D^2 - 4\chi_R \dot{Q}'/\lambda}] \quad (61)$$

$$\phi_o' = 0, \quad (62)$$

and

$$\phi_p = \lambda x_u'. \quad (63)$$

The total heating flux going to the wall is the sum of the convective and radiative fluxes; above the flame tip, however, we may do better to use the experimental result, Eq.(23), rather than continuing to use these theoretical fluxes. Thus, for the burning wall,

$$\phi_{pw}(x,t) \approx \phi_f [x_f/x]^{2.3}, \quad x > x_f \quad (64)$$

where

$$\phi_f \equiv \phi_c(x_f) + \phi_{rp}(x_f); \quad (65)$$

the subscript pw stands for "pyrolyzing wall." Note that we assume that $\phi_{pw}(x) = 0$ for $x < 0$.

7.4 Flux from the combined flame

If the igniter is left on after the wall begins to burn, the flames will "merge" -- that is, there is no way to distinguish the fuel-vapor contributions from the burner and from pyrolysis, to the resulting flame; the flame will simply become larger. The problem is how, then, to characterize the flux from the resulting flame. There is no clear experimental guide as to how to do this, and so we will simply reason plausibly.

The flux from the merged flame is not a simple superposition of fluxes from the igniter flame plus that from the pyrolyzed vapors which are burning. For one thing, that would correspond to a flame of unchanged height, whereas in fact the flame length will vary according to Eqs(38) or (39). Moreover, the pyrolysis vapors now enter an already-moving plume (and one which also has a different temperature distribution).

Normally, ignition of the wall will first occur in the neighborhood of the peak in flux from the igniting flame; i.e., in the neighborhood of z_{\max} . We expect the subsequent effects of combustion of the pyrolysis vapors to produce only a minor perturbation of the burner flux, at first.

We hypothesize that the combined flux is given by

$$\phi_w(z) \approx \Theta \phi_{wb}(z) + (1-\Theta)\phi_{pw}(z) \quad (66)$$

for the wall flux, where

$$\Theta \equiv \frac{\dot{Q}_b}{\dot{Q}_b + \dot{Q}_w} \quad (67)$$

and both ϕ_{wb} and ϕ_{pw} are each taken as if each separately produced \dot{Q}_{tot} ,

$$\dot{Q}_{tot} \equiv \dot{Q}_b + \dot{Q}_w \quad (68)$$

Consider the burner flux ϕ_{wb} , first: Eq.(42) was written as it was because we need the freedom to place X_m where we want. When there is pyrolysis, we expect that $X_m \approx X_p$, rather than $X_f/3$. In that case, Eq.(44) yields

$$B' = 1/2X_p \quad (69)$$

rather than (45), and Eq.(46) (modified slightly) yields

$$\lambda' = \frac{\ln 4}{X_f' - X_m} \approx \frac{1.386}{X_f' - X_p} \quad (70)$$

The new flame length, X_f' , is given by

$$X_f' = 0.14 \sqrt{\dot{Q}_b' + \dot{Q}_w'} \quad (71)$$

where \dot{Q}_b is the power output from the burner, \dot{Q}_w that from the combusting pyrolysis vapors. Note that (as is also true for m) dQ_b/dt may be a function of time. Also note that $\dot{Q}_w = \chi_A \Delta H_c \dot{m}$. Thus,

as the pyrolysis rate gradually increases, the flame length does too, and so do the magnitude and position of the radiation peak.

Finally, Eq.(47) becomes

$$F' = \frac{\bar{\chi}_R \dot{Q}'}{X_m [2X_m/3 + (X'_f - X_p) / \ln 4]} = \frac{1.386 \bar{\chi}_R \dot{Q}'}{X_p [X'_f - 0.0758 X_p]} \quad (72)$$

where

$$\bar{\chi}_R \dot{Q}' \equiv \chi_{R'} \dot{Q}'_b + \chi_{R'} \dot{Q}'_w \quad (73)$$

($\chi_{R'}$ is the radiant fraction from the pyrolysis vapors; it may differ from that from the burner gas(es), χ_R).

Note that one set of expressions is written in terms of X , with the burner height (z_b) as the origin, while the other is written in terms of x , with the bottom of the pyrolysis zone (z_{pb}) as the origin. When these are used together, as in Eq.(66), we must use a single coordinate system. One possibility is to use z (with the floor as the datum). Another is to note that since z_b is assumed to remain fixed, the one centered on it is the proper one to use. Then we must replace the x 's, in Section 7.3.2, by $X + z_b - z_{pb}$.

7.5 Flame heights and flame splitting

The power output is proportional to the mass-loss rate, and the latter is approximately proportional to the pyrolysis height, x_p . On the other hand, the flame height is only proportional to a fractional power of dQ/dt (see Eqs.(38) and (39)). Therefore, for sufficiently large values of x_p , Eqs.(38) or (39) will predict flame heights which are smaller than x_p . This is unphysical. A study (to be published) was carried out of how wall flame heights are influenced by x_p ; the result is

$$x_f \approx [x_{fo}^4 + x_p^4]^{0.25} \quad (74)$$

where x_{fo} is the flame height given by Eq.(38) or (39); that is, for a line burner against a wall. This is the expression now used in the program.

If the burning slab is thin, then the lower portions will burn through while the upper parts are still burning. If the burnt-through section is large enough -- that is, the lower pyrolysis front is sufficiently high, it will lie substantially above the (igniting) burner flame tip. Thus the flame will have split into two, and the burner flame will have negligible effect on the wall flame. The program handles this contingency.

8. MODEL EVALUATION

The first thing that needs to be validated is the assumption made (in Section 5) that h_g (the heat of gasification) is a valid "signature" for a material. In Fig.6, the $h_g(t)$ curves for Douglas fir plywood, found for $\phi_{ext} = 35$ and 65 kW/m^2 , are displayed. We note that they are indeed similar, in spite of the

large difference in the irradiation flux. The comparison, however, is not entirely appropriate: evidently the wood which is exposed to the higher flux will pyrolyze faster, so that "equivalent" points on the curves correspond to different times. This problem can be addressed in two ways: first, we could plot the curve against a time which is normalized by dividing t by the total duration of the burn. A more "physical" way, which does not depend on having a constant heating flux or on burning a thick specimen all the way through, is to plot against μ , the amount of mass per unit area which has been removed. Evidently μ is an implicit function of t , whose precise form depends on the flux impingement history.

In Figs.7 to 9, this has been done for exposures of 35, 65, and 85 kW/m², respectively. The curves should be "read" from right to left. It is apparent that much of the "noise" in Fig.6 has disappeared. It is also apparent that all three curves have a generic similarity, although there are some significant differences which will require elucidation before the technique can be used with maximal confidence. The negative values appear because some char oxidation begins to take place near the end. More convincing demonstrations of the uniqueness of h_g are given in Janssens (1991a) and in Urbas (1993).

Next, consider the performance of the program itself. Detailed comparisons have been carried out for PMMA and for wood (particle board). The input values for k , ρ , and c are shown in Table 1. For PMMA, the experimental results obtained by Orloff *et al* (1975) are exceptionally well reproduced, using the LIFT result for G-type PMMA: $k\rho c = 1.02$ (kW/m²K)²s; the figure showing this (Mitler, 1990) is reproduced here as Fig.10. We note, in Table 1, that the product of the ambient values gives the substantially smaller value $k\rho c = 0.357$ (kW/m²K)²s. This is not surprising, since both k and c increase with temperature. The LIFT value has been reproduced by multiplying the ambient values of k and c by about 1.7 each.

Table 1. Measured and estimated values of k , ρ , and c . The last two rows give the values actually used in the model; see the text for the origins of these values. The units for k , ρ , and c are W/m-K, kg/m ³ , and kJ/kg, respectively. For the product $k\rho c$, the units are (kW/m ² K) ² s								
Source	PMMA				Union Camp Particle Board			
	k	ρ	c	$k\rho c$	k	ρ	c	$k\rho c$
Ambient	0.209	1170	1460	0.357	0.124	670	1110	0.0922
LIFT				1.02				0.65
see text	0.346	1180	2500	1.02	0.204	670	1822	0.249
see text	0.311	1180	2250	0.83				

A similar experiment, but carried out with a much larger igniting burner (the burner strength was 47 kW/m) and without side rails to ensure two-dimensionality, was carried out more recently at NIST; those data are shown in Fig.11, with the fit as shown. The values used for k and c are each about 10% smaller than the previously chosen values, and thus about 1.5 times their ambient values; they yield $k\rho c = 0.83$ (kW/m²K)²s, within experimental error of the LIFT value. The method used for choosing these

values is discussed in the following section (Section 9).

In the Orloff *et al* experiment, the height of the front moved up as

$$x_p(t) \approx x_p(0) \exp(qt), \quad q = 0.0036 \text{ sec}^{-1};$$

In the NIST experiment (carried out by Steckler), $q = 0.0032 \text{ sec}^{-1}$.

For wood, Union Camp particle board was used; it was ignited by a 25.6 kW/m burner. Since k and c_p both rise with temperature, as is the case for PMMA, mean values of k and c must be used. Indeed, use of the ambient values of k (0.124 W/m°C), ρ (670 kg/m³), and c (1110 J/g) gives, as one might expect, overly rapid ignition ($t_{ig} \approx 52 \text{ sec}$, versus the experimentally-observed $t_{ig} \approx 70 \text{ sec}$, and a value of x_p at $t=600 \text{ sec}$ of about 65 cm (average value) or 78 cm (peak value)).

Using the "prescription" given in the next section, one easily finds the mean values for k and c shown in Table 1. Use of the value $T_{ig} = 405^\circ\text{C}$, as measured by LIFT, gives an ignition time about 25 s longer than observed. By assuming the slightly lower value $T_{ig} = 397^\circ\text{C}$, instead, one obtains the result shown in Fig.13: $t_{ig} \approx 100 \text{ s}$, and $x_p(600) = 83 \text{ cm}$. The fit to the data is reasonably good. The asymptotic height to which the pyrolysis front (on average -- see the filled circles in Fig. 13) is about 17 cm less than predicted. The relevant $k\rho c$ values are shown in Table 1. The input data file for PMMA is shown in Appendix A, that for Union Camp particle board in Fig.12.

9. OBTAINING THE INPUT DATA

The input data k , ρ , and c must be obtained either from the literature, or from (bench-scale) tests. When k and c are available from the literature, however, it is most often only at the ambient temperature. It has been found (Steckler *et al*, 1991) that when $k(T)$ and $c_p(T)$ are available from T_{amb} to T_{ign} , then good results are obtained, for PMMA, by taking k and c_p to be constant at the values they take on at the mean temperature $\langle T \rangle = (T_a + T_{ig})/2$.

For PMMA, $k(T)$ and $c_p(T)$ are known as functions of T , and the value at $\langle T \rangle = (T_a + T_{ig})/2 = (298+630)/2 = 464 \text{ K}$ was chosen for each, in the calculation shown: $c_p = 2250 \text{ J/g}$ and $k = 0.311 \text{ W/m-K}$.

Next, consider the Union Camp particle board; Parker (1988) gives the temperature dependencies of k and c_p for wood; they each vary approximately linearly with the absolute temperature, so that the thermal diffusivity is about constant. With the ambient values of k and c as given in Table 1, and an ignition temperature of about 400°C , we then find $\langle k \rangle = 0.204$ and $\langle c \rangle = 1822$.

Usually, k , ρ and c are not needed independently, but as the product $k\rho c$ (in calculating $T_{ig}(t)$, and for Eq.(2)). The LIFT apparatus yields $k\rho c$, Φ , and T_{ig} . Φ is needed for the calculation of the lateral spread rate, according to Eq(2); the value found from the LIFT apparatus is the correct one to use. It has been shown, however (Janssens, 1990/91), that the standard way of extracting $\langle k\rho c \rangle$ from the raw data tends to give too large an estimate for it; sometimes by a factor of two. Janssens (1990/91) has outlined a procedure by which one can obtain a more nearly accurate value of $\langle k\rho c \rangle$ from the raw data. If the original data are unavailable, however, one can only assume that the appropriate value to use is some submultiple of the value obtained from the LIFT apparatus.

Thus, for PMMA, the appropriate value is 80% of that given by LIFT. For the Union Camp particle board, LIFT gave $\langle k\rho c \rangle \approx 7A$ (where, again, A is defined as $A \equiv k\rho c$ at ambient temperature), whereas the appropriate value, 0.249, is only 2.7 times A .

Thus the procedure to be used is: when $k(T)$ and $c(T)$ are available (from T_{amb} to T_{ign}), use the average values. When they are not available, but a LIFT value is available, including the data from which it is obtained, use Janssens' method to get a better value. If the LIFT value is available, but not the data from which it is obtained, the situation is then highly unsatisfactory. As rational a procedure as any other, perhaps, is to take the geometric mean between the LIFT value and the ambient value; this works reasonably well for the particle board, but that may be fortuitous: it does not work so well for PMMA.

Next, consider χ_R , the radiative fraction. This is needed for the radiative flux distribution from the flame. This is the only datum for which there is no standard measurement method. There are a number of ways of measuring this global quantity; the most direct, involving the measurement of the radiation flux per steradian from the flame (the radiant intensity) in a number of different directions around the flame, is also the most difficult and time-consuming to carry out. Alternatively, we can measure the smoke-point length ℓ_s for the given material, and estimate χ_R based on the correlation between them found by Tewarson (1988): see Fig.14. FMRC has developed two apparatus which will measure ℓ_s routinely. Finally, one could eschew the measurement of ℓ_s entirely, and estimate χ_R from a measurement of χ_A (the completeness of combustion) based on the correlation of χ_A with ℓ_s also shown in Fig.14.

Finally, for the calculation of dm''/dt , the mass-loss rate measured at a specified irradiation level in the Cone Calorimeter (dm_c''/dt) must be found (Babrauskas, 1984). There are some difficulties with these measurements; perhaps the most significant one is that when the sample is held in place with a metal frame, which is the usual method, there are significant heat losses from the edges of the sample (Urbas, 1988). These losses can lead to underestimates of the mass-loss rate as great as 30%, so care must be taken in the measurement.

Still another point must be noted, in the interpretation of the results from the Cone: when the heater is calibrated, the flux read by the gauge is that due to radiation from the heater coil, plus that due to convection from below. That turns out to be about 13.6% of the total. Therefore, when the Cone is set to read 25 kW/m^2 , the radiation flux reaching the sample surface is actually only about 21.6 kW/m^2 . Another problem is that dm''/dt is calculated, in the experiment, by numerical differentiation of $m''(t)$. The mass measurement, however,

- a. requires some corrections, such as for buoyancy, and
- b. it is a "noisy" measurement, so that the derivatives are poor.

One way to get around these difficulties is to measure dQ/dt , the rate of heat release. This is an integral measurement, so that the errors due to numerical differentiation of a function defined by points exhibiting considerable statistical scatter, as suggested by (b) above, disappear. It also avoids any buoyancy difficulties.

10. USERS' GUIDE

SPREAD is available on a diskette for IBM-PC-compatible computers (note: NIST does not endorse any particular commercial product). The distribution diskette includes both executable and source code for SPREAD, as well as sample input files. It also includes a simple plotting program, PLOTBOTH, which

can be used to show the upper and lower pyrolysis front heights as a function of time, once the calculation has been completed. SPREAD requires a 386 class PC or better, preferably with math coprocessor. Typical execution times on a 33MHz 486 computer are about 6% of real time; thus, about 40 seconds for a 600-second simulation.

It is best to create a single subdirectory for the executable programs and related data files; this will allow you to easily delete all the files related to this program when you are finished with it. In general, when running on a PC, keep all files in the current working directory.

When used as a stand-alone program, SPREAD is quite easy to use: upon typing the word SPREAD, a series of questions will appear on the screen, requesting information. One has merely to follow the instructions appearing on the screen. The first screen is the following (it is italicized here only to distinguish it from the rest of the text):

Wall/slab data may be entered in the following ways:

(1) By typing it in at the keyboard.

(2) By reading it from a file.

Please enter the number of your choice:

If "1" is typed, then a series of questions will appear, requesting information. The information pertains to the slab (its geometry, thermophysical properties), the ambient conditions, the length of the run, etc. The first question is for the wall/slab height; the second for the height of the bottom of the slab above the floor; the third, for the slab density, and so forth. The requested data, in the correct order, is indicated by the left-hand side of the first list in Appendix A.

It is much easier to input all that information by typing in the name of an input file (examples are given in the text). For input *via* a prepared file, press "2", then "enter"; the user is then requested to give the name of the file. The information read from the file is then echoed, in its entirety, on the screen. Note: one cannot do both -- i.e., enter a few input values and then the rest *via* an input file.

When all the data has been entered (*via* the keyboard or *via* a file) and read, the following second general request will appear on the screen:

Mass-loss rate data may be entered in the following ways:

(1) By typing it in at the keyboard.

(2) By reading it from a file.

(3) By an internal calculation.

!!! Note: Option 3 has been deactivated. !!!

Please enter the number of your choice:

The same remarks apply as for the first question. This second data request is for mass-loss rate data from the Cone Calorimeter. An example is given by the second list in Appendix A (top of the second page there). Note that the "mass-loss rate" data is actually power output from the cone (in kW/m²) (this becomes evident from the program if "1" is chosen as the option).

The third screen is not displayed here, as it is very similar to the first two; it requests data pertaining to the igniting (line) burner. (Here, it is not even necessary to invoke option 1 to see what the contents are: the contents are echoed in their entirety on the screen, upon typing in the file name). They are also indicated by the third list in Appendix A.

Finally, a request is made for the wall-temperature and external flux data. The temperatures of the upper and lower parts of the wall (outside of the flaming and preheating regions, that is) are needed for the lateral-growth part of the program. This is somewhat redundant, since the wall temperatures were already requested in the first list shown; although this redundancy has survived the development of the program, it presents no difficulties. The external flux data are needed for both the upward and lateral spread calculations. *Be sure to enter the wall temperatures in degrees Kelvin, not °C.!*

After all the needed data have been input, the program requests that the user give a name to "the" output file (there are five output files, only one of which is named by the user). Assume the user chooses the name YOURFILE.NAM. Calculation then proceeds forthwith. There is no opportunity to return and fix any errors -- the program just runs. If it is desired that the calculation be interrupted at any point, ^S (control-S) can be typed; calculation can be resumed by typing ^R. If it is decided to abort the calculation, typing ^C twice will stop it entirely. There is no screen output while the heat-up to ignition is being calculated. Once ignition occurs, there's screen output. One will note, on the screen, "real" time t, followed by "IGTIME," which is the time from first ignition. Finally, XP1, which is the height of the upper pyrolysis front. The last screen output is PHROUT, the outward flux at each node (this includes the flame flux and surface radiation).

The results are placed in five files: YOURFILE.NAM (our putative choice for the output file), TEMPS, JUNK, SPREAD.PLT, and WALLPLOT.DAT. YOURFILE.NAM contains most of the interesting information. There,

S is the time step, in seconds

Xp1 is the position of the upper pyrolysis front (in meters)

Xpb1 is the position of the lower pyrolysis front [m]

M and L can be ignored (these are fossil remnants of the debugging process)

The mass-loss rate in the pyrolyzing region, in g/m²-sec

Q_{dot}(W+B) is the power output of the burner plus that of the wall, in Watts

Xps = Xp1 - Xs (Xs = position of burner above floor) [m]

Xf = flame-tip height [m], and

Xp = Xp1 - Xpb1 = vertical extent of pyrolysis zone, also in meters.

TEMPS principally contains the surface temperature at every node, for several times: just at ignition, then at multiples of 100 sec beyond that. Note that -- except at ignition -- the pyrolyzing nodes are all at the "ignition" temperature (this file, too, is a fossil remnant).

JUNK is there mostly for debugging purposes. It contains $\xi(t)$, $\tau_1(t)$, cone mass-loss rate, etc. ξ and τ are explained in Section 5; this output can be ignored.

SPREAD.PLT is output for a plotting program such as SIGMAPLOT (this software is used as an example only; NIST does not endorse any particular commercial product).

WALLPLOT.DAT is used by the ancillary program PLOTBOTH.EXE, to produce a graph of the results [$x_p(t)$ and $x_{pb}(t)$]. (It can also be used by WALLPLOT.EXE, another ancillary graphics program, not included in this package). In order to see the graph displayed, simply type "plotboth" after the main program has been executed.

There are, in principle, no limits to the domain variables the user may specify; however, the number of horizontal slices into which the wall is divided is limited to 100. Hence a 100-meter high wall, for

example, will have nodes one meter apart, which will lead to extremely crude calculations. Again, as has been noted in Sections 8 and 9, the results of the calculations are very sensitive to some of the input parameters, such as the ignition temperature of the wall material: taking the ignition temperature to be just 10°C higher than that assumed for the calculation shown in Fig. 13 (an increase of 1.5%), moves the entire calculated curve down and to the right, with ignition at $t = 124$ s (at the same height), and a pyrolysis front height 8 cm lower at $t = 600$ (75 cm vs 83.2 cm). The sensitivity to the $k\rho c$ input is also substantial, though not as extreme: a 27% reduction in $k\rho c$ results in shifting the curve in the other direction (to the left and up), with ignition at $t = 76$ s.

Note: it is possible to treat the case of autoignition due to exposure to high radiation levels, but without a pilot (igniter) flame, with this program. In order to do this, one needs to use the *autoignition* temperature (the usual "ignition temperature" refers to piloted ignition). Once ignition has been achieved, the program must be interrupted, and then run a second time, using the usual ignition temperature. In order to get the spread rate correctly, one would assume, for the second run, the existence of an igniting burner whose flame is large enough to more than cover the area which is made to ignite by the actual radiant flux, plus an effective external flux. The magnitude of this flux must be such that the sum of it, plus the total heating flux from the virtual burner, combine to equal the actual large external flux.

11. SUMMARY

The computer program SPREAD calculates the upward spread rate and burning intensity on a flat wall for (in principle) arbitrary materials. It has been validated against one ablating and one charring material (PMMA and particle board, respectively), where SPREAD has performed reasonably well. The calculation is numerical, rather than analytic, and assumes the existence of a unique "ignition temperature." The pyrolysis rate varies from point to point; it depends on the wall material properties as well as on the (local) heating flux, from convection and from radiation. A special transformation is used to translate Cone Calorimeter pyrolysis results obtained at any radiation level, to find what the mass-loss rate is for any other exposure, in the real fire. Regression of the surface is explicitly taken into account, and the possible resulting burnthrough. Lateral (creeping) spread on the wall is calculated as well; the lateral-spread calculations have not been validated, however.

The heating fluxes from the flame are internally calculated; the radiant contribution is based in part on the global radiation fraction. The radiation flux includes any external fluxes, as well as from the flame. The contributions from any igniter or burner are added to those from pyrolysis, to arrive at the total power output and flame flux. The effects of a ceiling on vertical or lateral wall flame spread have not been taken into account, nor that of burning with hot and/or vitiated air as the oxidant.

There are two help sections for the user: one on how to obtain input data for the program, and a Program Users' Guide. Several appendices give details which are important for the user, as well as details about the program and its structure, to enable a user to make changes in the program, should he/she wish to do so.

12. ACKNOWLEDGEMENT

The authors wish to express their sincere appreciation for the excellent work done by Ms. Marjorie McClain in reprogramming, streamlining, and extending the program SPREAD.

REFERENCES

- Ahmad, T., and Faeth, G.M. (1978) "An Investigation of the Laminar Overfire Region Along Upright Surfaces," *J. Heat Transfer* **100**, p. 112
- Ahmad, T., and Faeth, G.M. (1979) "Turbulent Wall Fires," in the 17th Symposium (International) on Combustion, The Combustion Institute, Pittsburgh, PA, p. 1149
- Atreya, A. (1983) "Pyrolysis, Ignition, and Fire Spread on Horizontal Surfaces of Wood," Ph.D. Thesis, Harvard University, Cambridge, MA, May 1983
- Babrauskas, V. (1984) "Development of the Cone Calorimeter -- a bench-scale heat release rate apparatus based on oxygen consumption," *Fire and Materials* **8**, No.2, p.81
- Cleary, T.G., and Quintiere, J.G. (1991) "A Framework for Utilizing Fire Property Tests," *Fire Safety Science, Proceedings of the Third International Symposium*; Eds. G. Cox and B. Langford; Elsevier Applied Science, N.Y. p. 647
- de Ris, J.N. (1969) "Spread of a Laminar Diffusion Flame," in 12th Symposium (International) on Combustion, the Combustion Institute, Pittsburgh, PA, p.241
- de Ris, J.N. (1979) "Radiation - A Review," in 17th (International) Symposium on Combustion; the Combustion Institute, Pittsburgh, PA, p.1003
- Hasemi, Y. (1986), "Thermal Modeling of Upward Wall Flame Spread", in *Fire Safety Science (Proceedings of the First International Symposium)*; eds., C.E. Grant and P.J. Pagni; Hemisphere Publishing Corp., p.87
- Holman, J.P. (1981), **Heat Transfer** (5th ed.), McGraw-Hill, N.Y.
- Janssens, M. (1991) "A Thermal Model for Piloted Ignition of Wood, Including Variable Thermophysical Properties," *Fire Safety Science, Proceedings of the Third International Symposium*; Eds. G. Cox and B. Langford; Elsevier Applied Science, N.Y. p. 167
- Janssens, M.L. (1991a) "Fundamental Thermophysical Characteristics of Wood and their Role in Enclosure Fire Growth," Ph.D. thesis; National Forest Products Association, Washington, DC 20036
- Karlsson, B. (1992) "Modeling Fire Growth on Combustible Lining Materials in Enclosures," report TVBB-1009, Dept. of Fire Safety Engineering, Lund University, Lund, Sweden (thesis)
- Kulkarni, A.K., Kim, C.I., and Kou, C.H. (1991) "Turbulent Upward Flame Spread for Burning Vertical Walls Made of Finite-Thickness, Practical Materials," Annual Report to NIST, May, 1991
- Kulkarni, A.K., and Kim, C.I. (1992) "Turbulent Upward Flame Spread on Vertical Walls," to be submitted to *Combustion and Flame* (10/92)
- Marxman, G.A. (1965) "Combustion in the Turbulent Boundary Layer on a Vaporizing Surface," Tenth Symposium (International) on Combustion, The Combustion Institute, Pittsburgh, PA, p.1337

Markstein, G.H. (1987) in May-Aug. 1987 Quarterly Progress Report for NBS Grant No. 60NANB5D0560 to Factory Mutual Research Corp.

Markstein, G.H. and de Ris, J. (1990), "Wall-Fire Radiant Emission, Part I: Slot-burner Flames; Comparison With Jet Flames," FMRC report RC-90-BT-2, Factory Mutual Research Corp., Norwood, Mass. Also in the 23d Symposium (International) on Combustion, The Combustion Institute, Pittsburgh, PA (1991), p. 1685

McCaffrey, B.J. (1979) "Purely Buoyant Diffusion Flames: Some Experimental Results," NBSIR 79-1910, Center for Fire Research, National Bureau of Standards, Gaithersburg MD, 20899

Mitler, H.E. (1986) "Exponential Spread Rate of Some Wall Fires," Ann. Conf. on Fire Research, National Bureau of Standards, Gaithersburg, MD, Nov. 1986

Mitler, H.E., and Rockett, J.A. (1987) "Users' Guide to FIRST, a Comprehensive Single-Room Fire Model", NBSIR 87-3595; National Bureau of Standards, Gaithersburg, MD, 1987.

Mitler, H.E. (1988), "Algorithm for the Mass-Loss Rate of a Burning Wall", NBSIR 87-3682; National Bureau of Standards, Gaithersburg, MD, 1987, and in Fire Safety Science - Proceedings of the Second International Symposium (Eds., C.E. Grant and P.J. Pagni); Hemisphere Publishing Corp.

Mitler, H.E. (1990) "Predicting the Spread Rates of Fires on Vertical Surfaces," 23d (International) Symposium on Combustion; The Combustion Institute, Pittsburgh, PA, p. 1715

Orloff, L., de Ris, J., and Markstein, G.H. (1975), "Upward Turbulent Fire Spread and Burning of Fuel Surfaces," in 15th (International) Symposium on Combustion; the Combustion Institute, Pittsburgh, PA, p.183

Orloff, L., Modak, A.T., and Alpert, R.L. (1977), "Burning of Large-Scale Vertical Surfaces"; in 16th International Symposium on Combustion; the Combustion Institute, Pittsburgh, PA, p.1345

Parker, W.J. (1985), "Prediction of the heat release rate of wood," Fire Safety Science - Proceedings of the First International Symposium (Eds., C.E. Grant and P.J. Pagni); Hemisphere Publishing Corp, pp.207-216

Parker, W.J. (1988) "Prediction of the Heat Release Rate of Wood," Ph.D. Thesis, George Washington University, Washington, D.C.

Quintiere, J.G. (1981) "An Approach to Modeling Wall Fire Spread in a Room", Fire Safety J. 3, p.201

Quintiere, J.G., Harkleroad, M., and Hasemi, Y. (1986) "Wall Flames and Implications for Upward Flame Spread", Comb. Sci. and Tech. 48, p.191

Quintiere, J.G. (1988), "The Application of Flame Spread Theory to Predict Material Performance," Journal of Res. of Nat'l Bur. of Standards 93, No.1, p.61

Saito, K., Quintiere, J.G., and Williams, F.A. (1985), "Upward Turbulent Flame Spread", Fire Safety Science - Proceedings of the First International Symposium (Eds., C.E. Grant and P.J. Pagni); Hemisphere Publishing Corp., p.75

Sibulkin, M., and Kim, J. (1977), "The Dependence of Flame Propagation on Surface Heat Transfer, II. Upward Burning", *Comb. Sci. and Technology* **17**, p.39

Spalding, D.B. (1953), "The Combustion of Liquid Fuels," in the 4th Symposium (International) on Combustion; the Combustion Institute, Pittsburgh, PA, p.847

Steckler, K.D., and Mitler, H.E. (1988) "Experimental Study of the Pyrolysis Rate of a PMMA Wall Panel in a Reduced-Scale Enclosure," Combustion Institute/Eastern States Section; Chemical and Physical Processes in Combustion; Technical Meeting, Clearwater Beach, Fla., 73/1-4 pp., Dec. 1988

Steckler, K.D., Kashiwagi, T., Baum, H.R., and Kanemaru, K. (1991) "Analytical model for transient gasification of noncharring thermoplastic materials," Proceedings of the Third International Symposium; Eds. G. Cox and B. Langford; Elsevier Applied Science, N.Y. p. 895

Steward, F.R. (1970), *Combustion Science and Technology* **2**, p.203

Tewarson, A., Lee, J.L., and Pion, R.F. (1980) "The Influence of Oxygen Concentration on Fuel Parameters", in 18th (International) Symposium on Combustion; the Combustion Institute, (1980) p.563

Tewarson, A. (1988) "Smoke point height and fire properties of materials," NIST-GCR-88-555, National Institute of Standards and Technology, Gaithersburg, MD 20899

Urbas, J. (1993) "Nondimensional Heat of Gasification Measurements in the Intermediate Scale Rate of Heat Release Apparatus," *Fire and Materials* **17**, p.119

Wickström, U., and Göransson, U. (1987) "Prediction of Heat Release Rates of Surface Materials in Large-Scale Fire Test Based on Cone Calorimeter Results," *ASTM Journal of Testing and Evaluation*, Vol.15, No.6

NOMENCLATURE

B	Spalding mass-transfer number; coefficient in Eq.(42)
B'	B, modified to take combustion efficiency and radiation into account
B _c	Convective B-number
c _p	Specific heat of air
c	Specific heat of material
F	Initial slope of radiative flux distribution from burner flame (see Eq.(42) ff.)
Gr	Grashof number
h	Heat-transfer coefficient
h _c	Convective heat-transfer coefficient
h _w	Height of the wall or slab under consideration
h _{wb}	h when there is "blowing"; see Eq.(33)
H _c	Lower heat of combustion
H _v	Effective (gross) heat of vaporization
k	Thermal conductivity of wall/slab material
$\dot{m} \equiv dm/dt$	Mass-loss rate of wall/slab
\dot{m}''	Pyrolysis (mass-loss) rate per unit area
\dot{m}_0''	Pyrolysis rate in the absence of radiation, as a function of x
N	Number of slices into which wall (or slab) is divided
\dot{Q}	Power output (RHR)
\dot{Q}'	Power output per unit width
t	Time
t ₀	Time at which ignition has started
T	(Absolute) temperature
T _c	Critical wall temperature for (lateral) spread
T _f	Mean flame temperature
T _g	Fuel gas temperature; generally the same as T _s
T _{ig}	Ignition temperature
T _j ^k	The temperature at node j, time t _k
T ₀	Initial (uniform) temperature of the wall/slab
T _p (z,t)	Mean temperature of the thermal plume at that height and time
T _s	Surface temperature; generally a function of time

V_s	Velocity of spread of pyrolysis front
w	Width of pyrolyzing area
x	Height above z_{pb} ; i.e., above base of flame
X	Distance above z_s ; i.e., above slot or line burner
x_f	Flame-tip height (above z_{pb})
x_p	Total height of pyrolyzing zone
$y_o = Y(O_2)$	Mass fraction of oxygen
z	Height above floor
z_b	Height of bottom of slab above the floor
z_f	Flame-tip height above floor
z_{max}	Height at which total wall heat flux is a maximum
z_M	Height of hot/cold layer interface
z_n	Position of nth node
z_p	Position of (advancing) pyrolysis front (at time t, that is)
z_{pb}	Position of bottom of pyrolysis zone; this front may initially progress downward to z_s . It then stays at z_s (which may or may not be at z_b) for a time, then regresses (upward) as the burnout front

Greek symbols

α_w	Absorptivity of the surface	
β	Coefficient for flame-height correlation (Eq.(38))	$[m^{5/3} kW^{-2/3}]$
β'	Coefficient for flame-height correlation (Eq.(39))	$[m^{3/2} kW^{-1/2}]$
Δt_s	Duration of time step s: $t_s - t_{s-1}$	[sec]
Δx	Height of slice of wall/slab	[m]
ϵ_w	Emissivity of the surface	
λ	Coefficient in Eq.(42)	
μ	Mass per unit area which has been pyrolyzed away	$[kg/m^2]$
Θ_i^s	Wall/slab thickness at (z_i, t_s)	[m]
Θ_0	Wall/slab thickness for uniform case	
ξ	Ratio of net fluxes; Eq.(20)	
ρ	Density of wall/slab material	$[kg/m^3]$
σ	Stefan-Boltzmann constant	
τ	Scaled time (in Cone Calorimeter)	[s]

ϕ	Generic symbol for energy flux	[kW/m ²]
ϕ_b	External heating flux striking bottom of pyrolysis zone	
ϕ_c	Convective heat flux	
ϕ_M	External heating flux which strikes pyrolyzing slab at its intersection with the layer interface height	
ϕ_r	Radiative heat flux	
ϕ_t	External heating flux striking top of pyrolysis zone	
ϕ_{ex}	External heat flux (not from the flame)	
$\phi_{f,c}$	Heat flux from flame, in the Cone Calorimeter (see Eq.(12))	
ϕ_{pw}	Total flux to wall from flames due to pyrolyzing wall (no burner)	
ϕ_{rf}	Radiative heat flux from the flame	
ϕ_{rp}	Radiation from flames due to pyrolyzing wall (no burner)	
ϕ_{rr}	Reradiation flux from the surface	
ϕ_{wb}	Total flux to wall from burner alone	
Φ	Lateral spread parameter; see Eq.(2)	
χ_A	Combustion efficiency of fuel	
χ_R	Fraction of flame's power output going into radiation	

Subscripts

a	Ambient
b	Bottom; burner
c	Convective; Cone
f	Flame; flame tip
g	Gas
o	Oxygen; value at origin; initial value
p	Pyrolysis; isobaric
r	Radiative
s	Surface
t	Total
v	Vaporization
w	Wall

Superscripts

s	Time-step index
---	-----------------

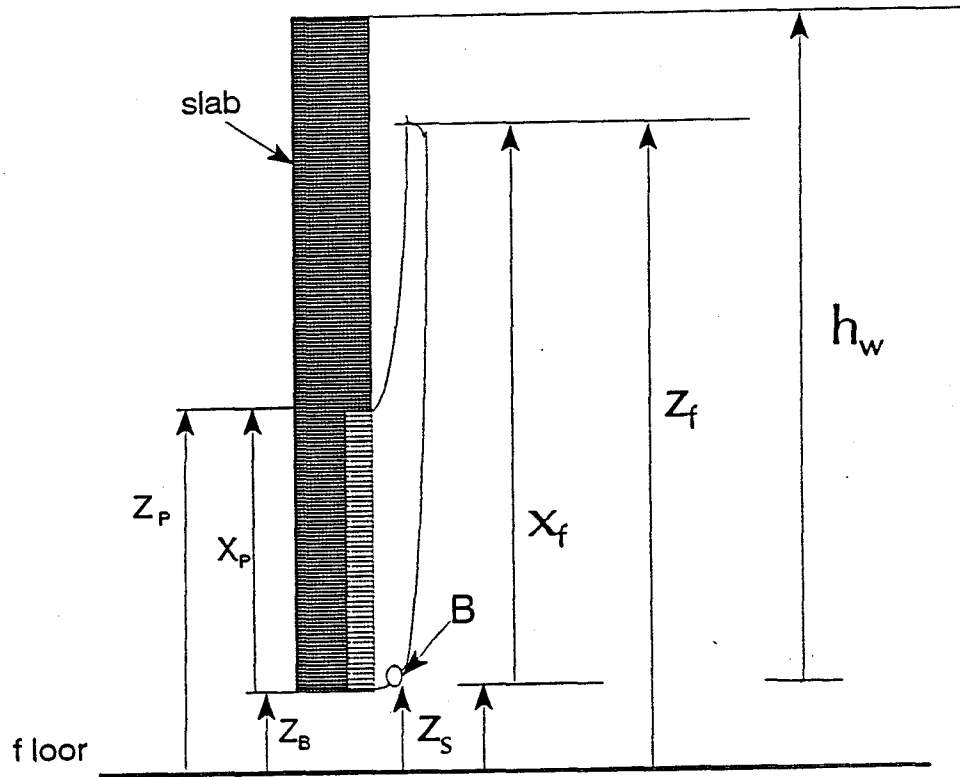


Figure 1a. Schematic of wall and wall flame. The igniter, a slot burner, is marked B. The igniter fuel and pyrolysis vapors mingle and result in a single "merged" flame. For simplicity, we have assumed that $Z_B = Z_S = Z_{PB}$. The shaded part of the slab is the pyrolyzing zone.

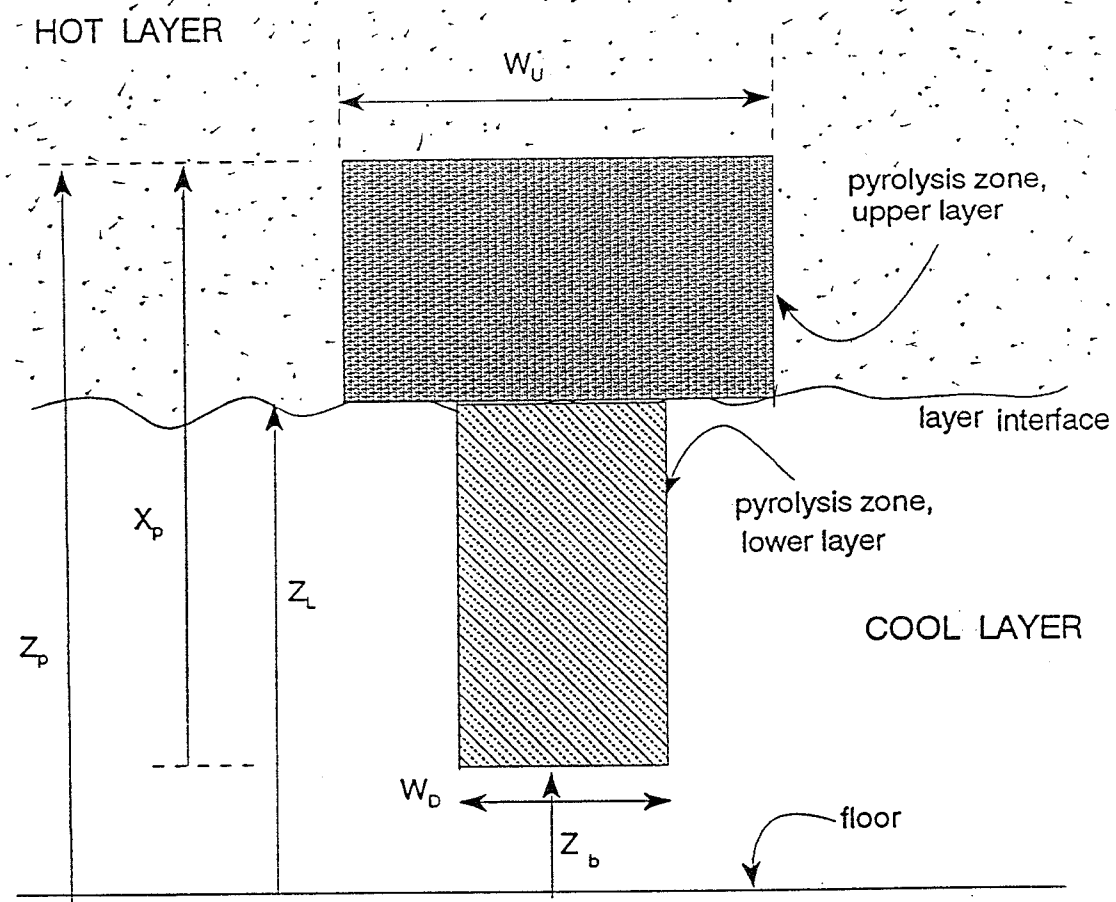


Figure 2. Idealized pyrolyzing area in a two-zone room-fire simulation.

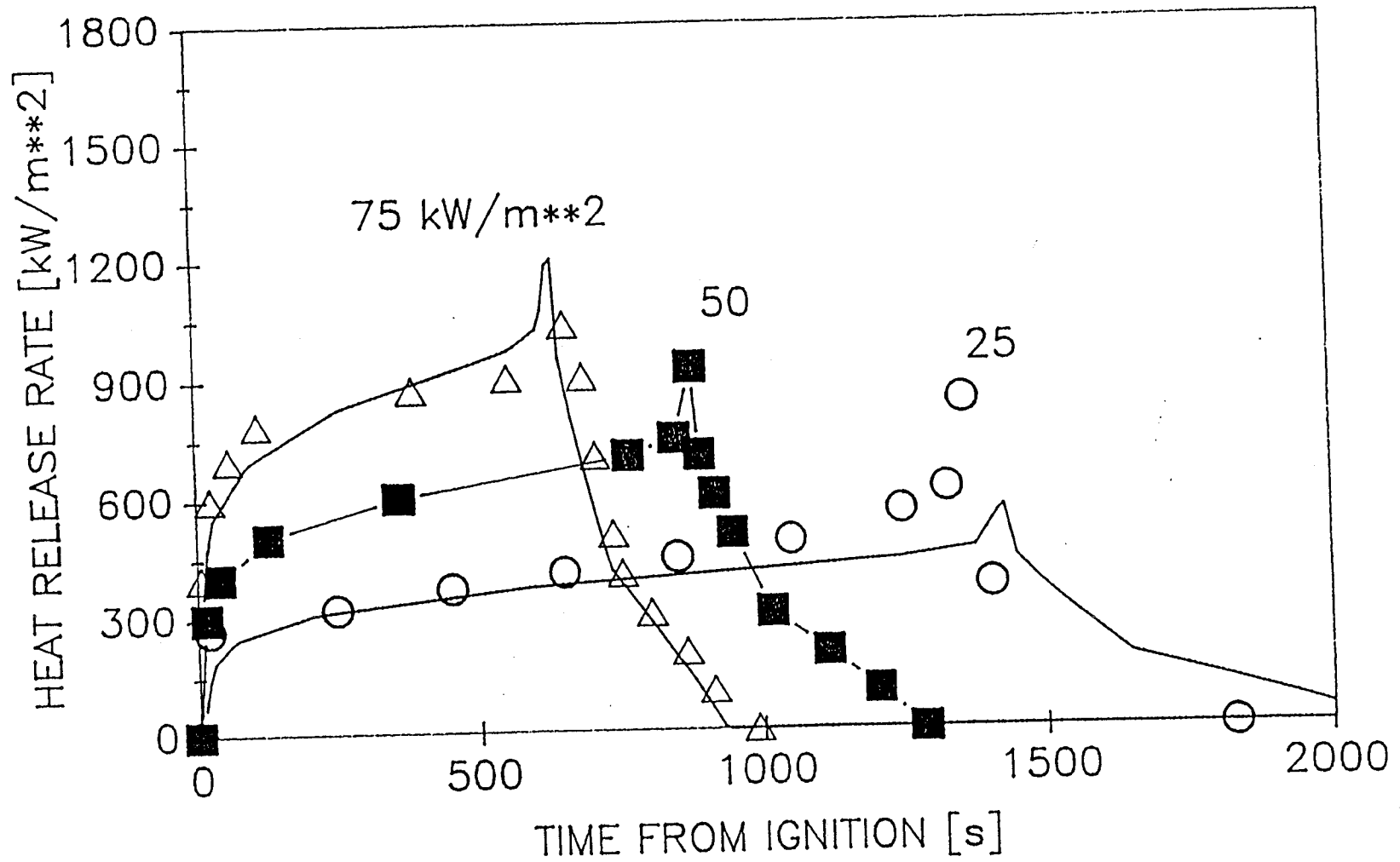


Figure 3. The mass-loss-rate data for PMMA, as obtained from the cone calorimeter, is given for several irradiation fluxes by the data points. See text for a description of the solid curves.

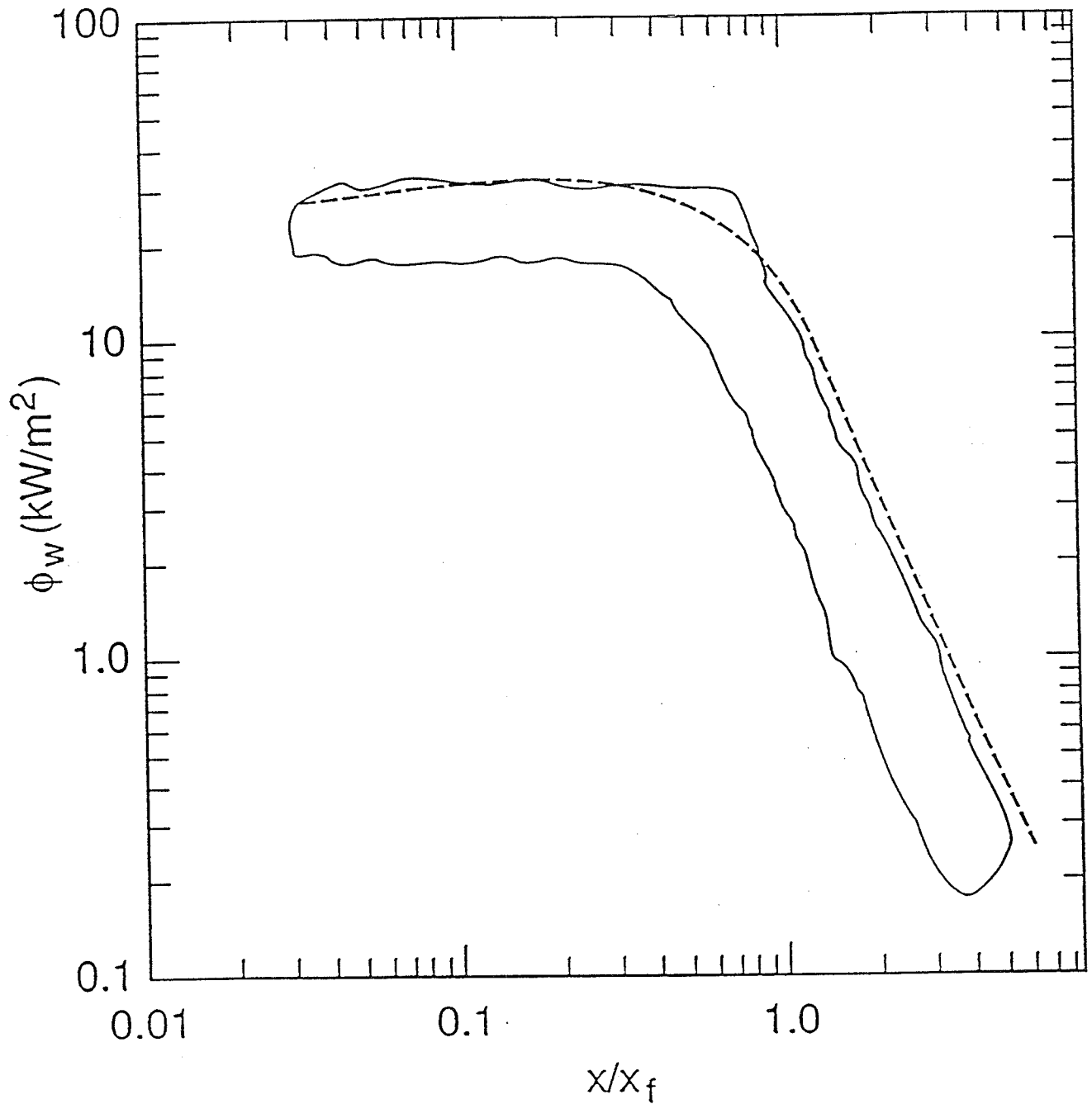


Figure 4. Measured (total, steady-state) fluxes from wall flames back to the wall. The envelope contains much of the available data. The dashed curve is the flux, calculated according to the formulation in this article, at $t = 0$ for a 4 kW slot burner. The abscissa is normalized by the flame heights.

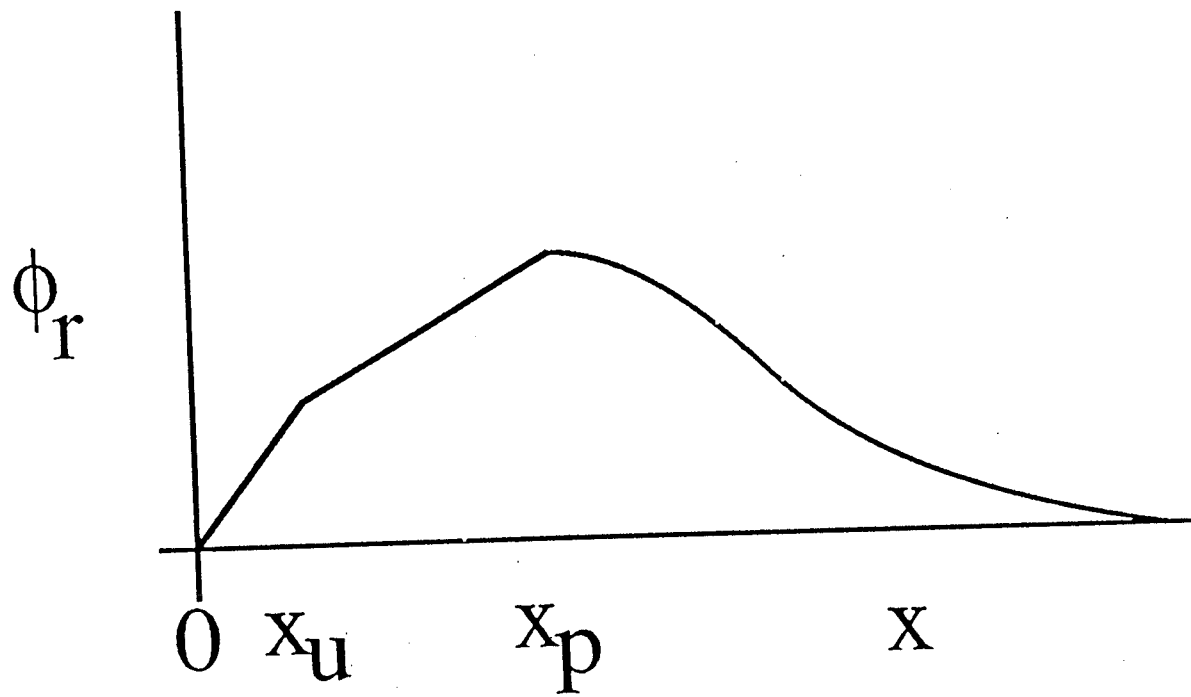


Figure 5. Schematic of the radiation flux from a burning-wall flame back to the wall, according to Eq.(50).

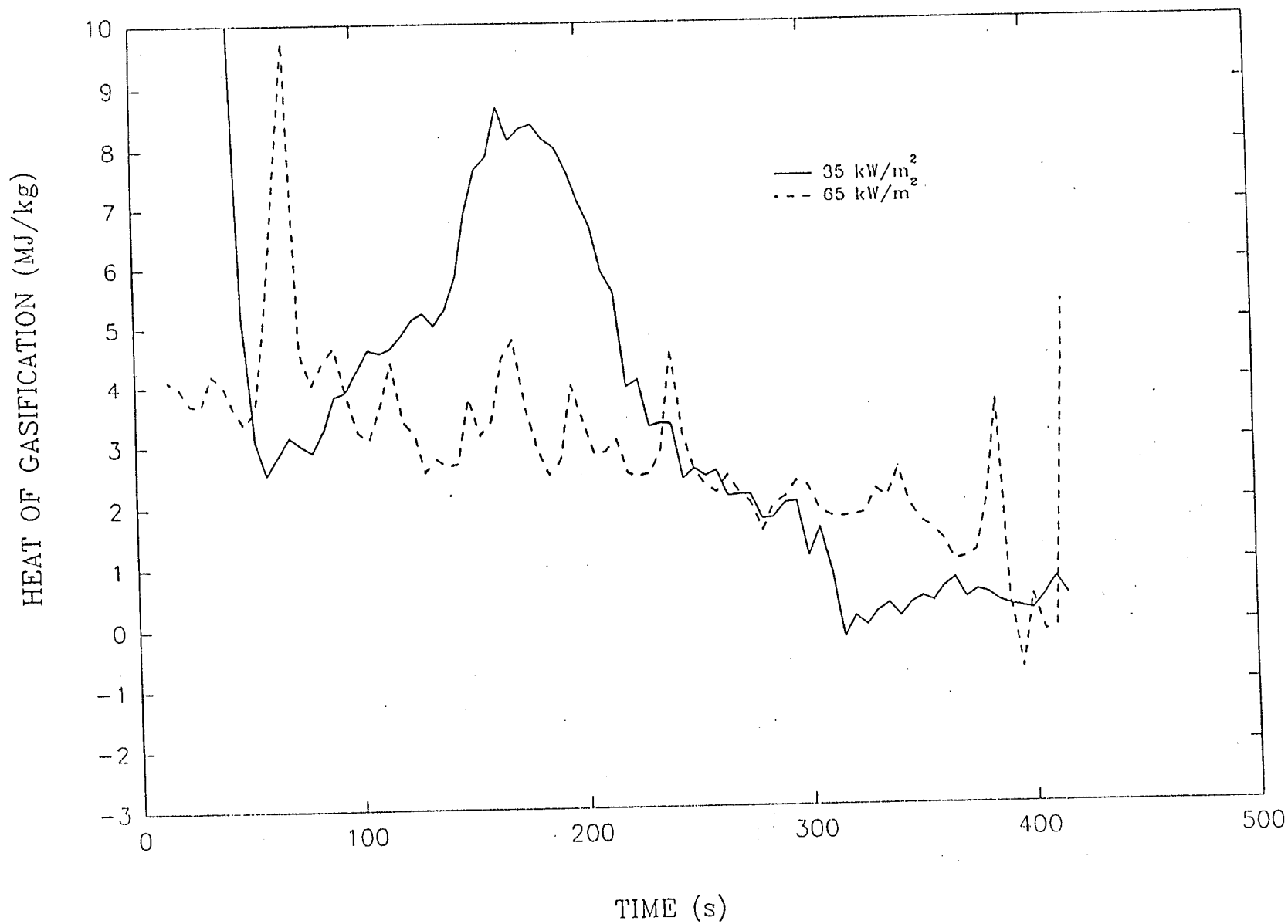


Figure 6. The time dependence of the heat of gasification, $h_g(t)$, of untreated Douglas fir plywood, irradiated at 35 and 65 kW/m². The measurements were made in the Cone Calorimeter.

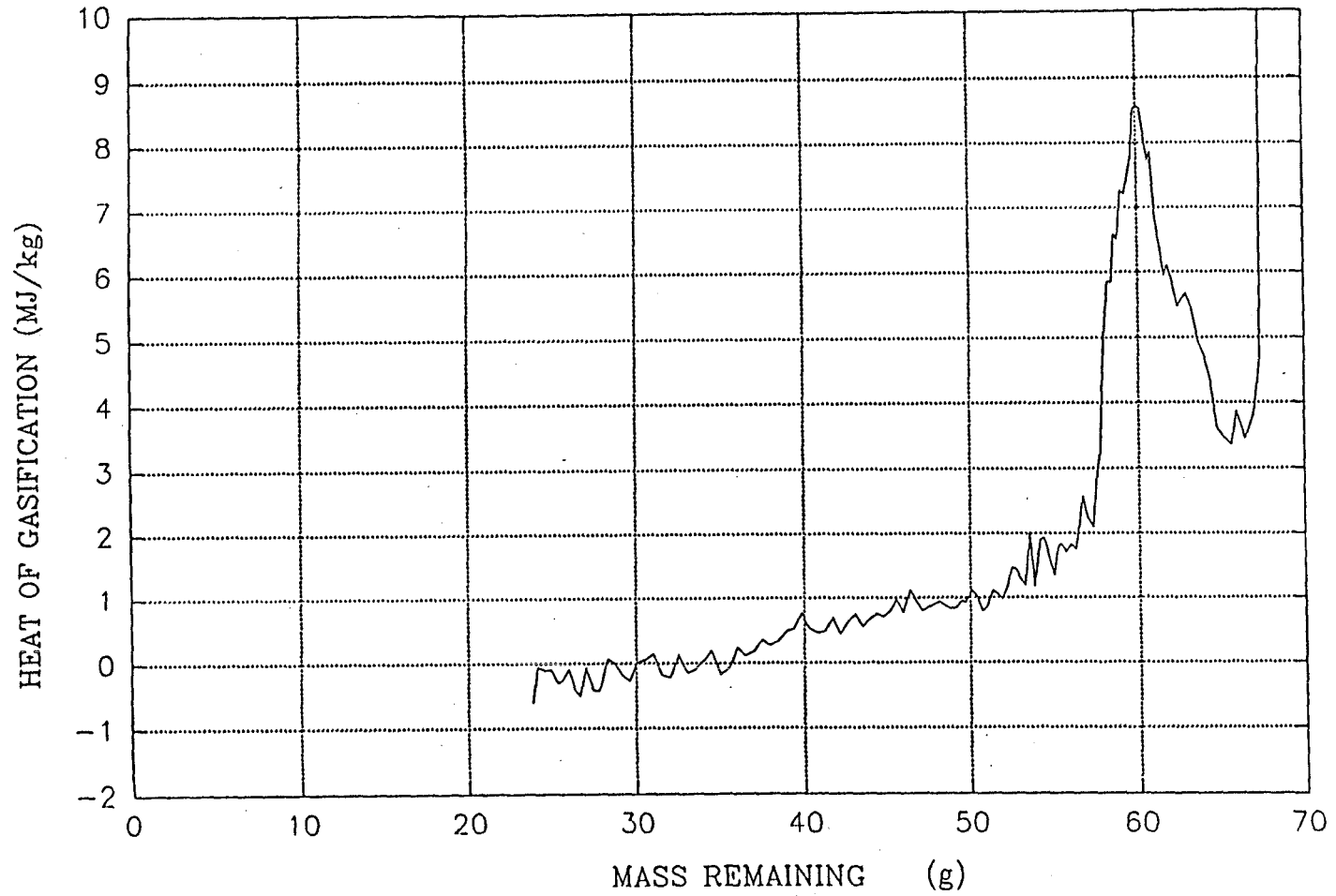


Figure 7. The heat of gasification of untreated Douglas fir plywood irradiated with 35 kW/m^2 , as a function of the remaining mass.

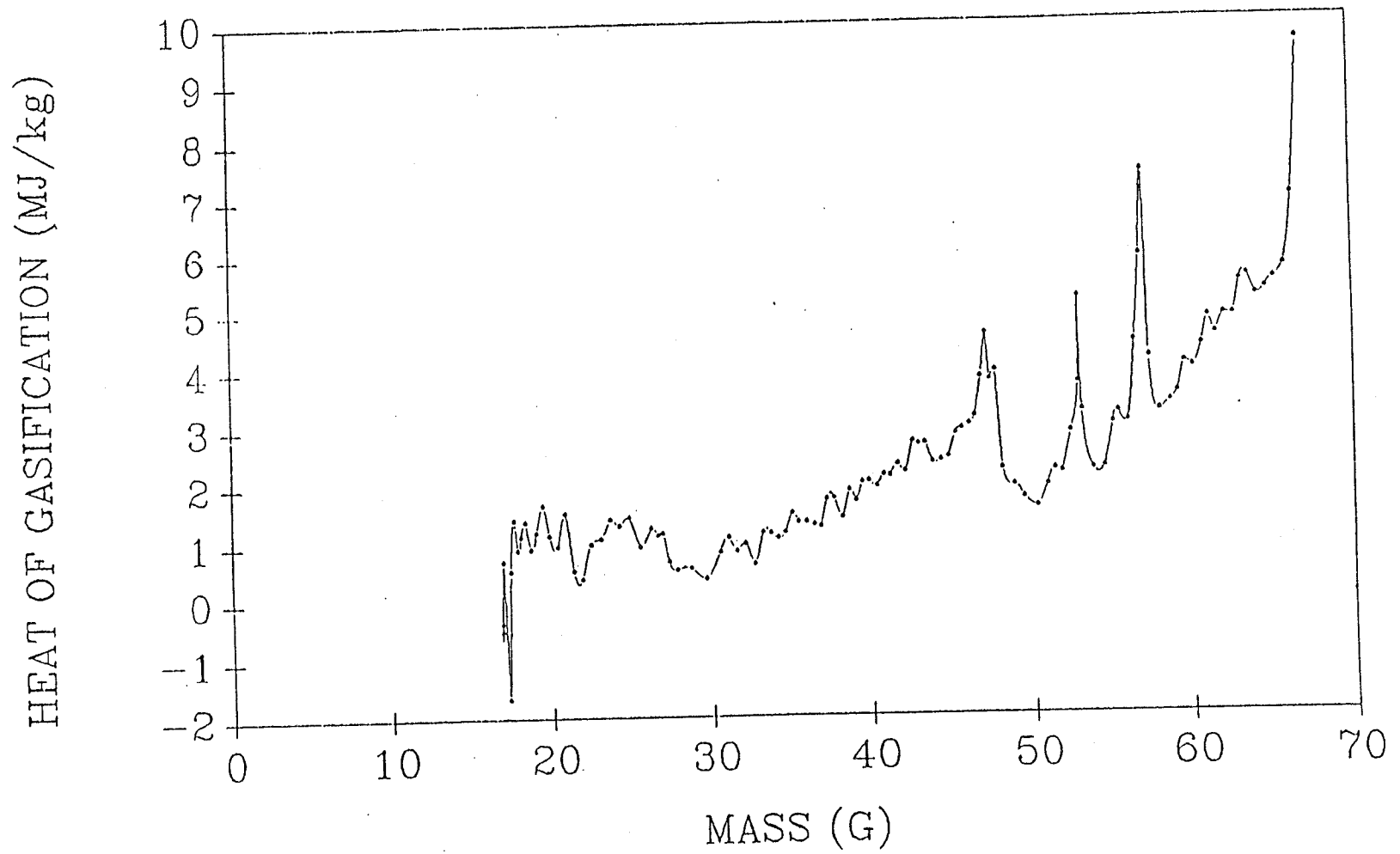


Figure 8. The heat of gasification of untreated Douglas fir plywood irradiated with 65 kW/m^2 , as a function of the remaining mass.

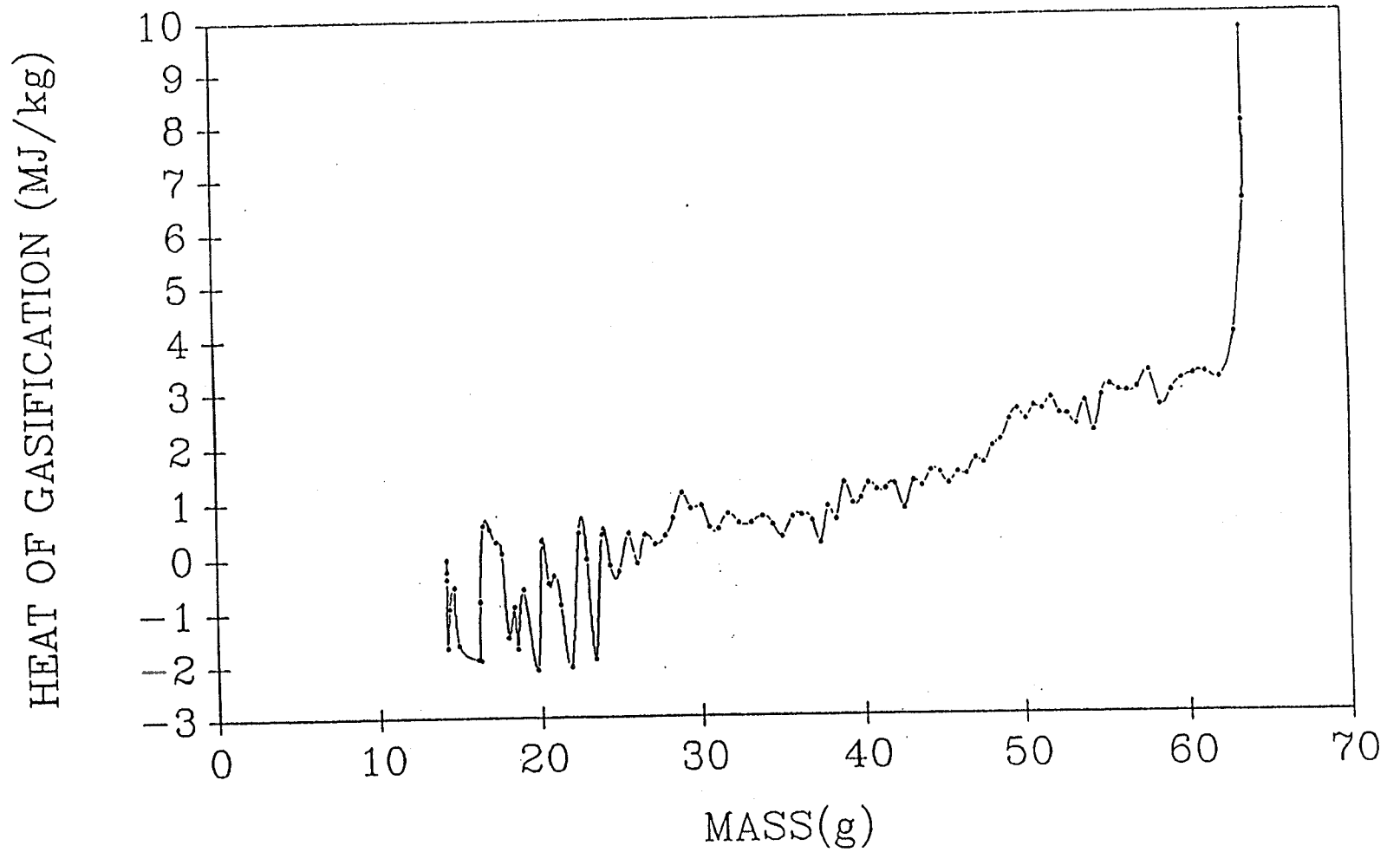


Figure 9. The heat of gasification of untreated Douglas fir plywood irradiated with 85 kW/m^2 , as a function of the remaining mass.

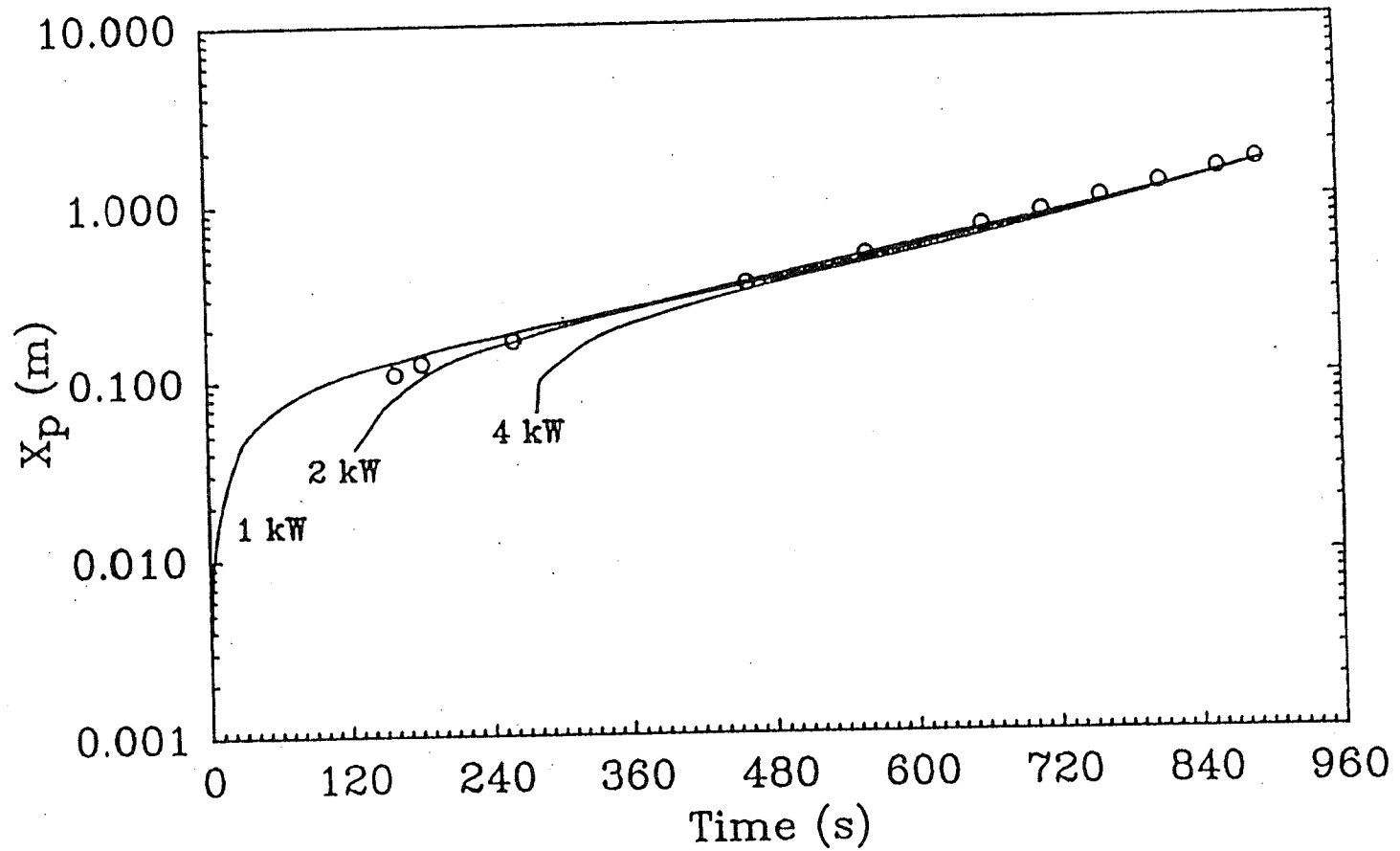


Figure 10. Position of the upper pyrolysis front as a function of time, for thermally-thick PMMA. Open circles are FMRC data; solid curves are calculated positions for several assumed burner strengths. The burner width is 0.4 m, so that Q_b must be multiplied by 2.5 to get Q' .

UPWARD FLAMESPREAD ON PMMA

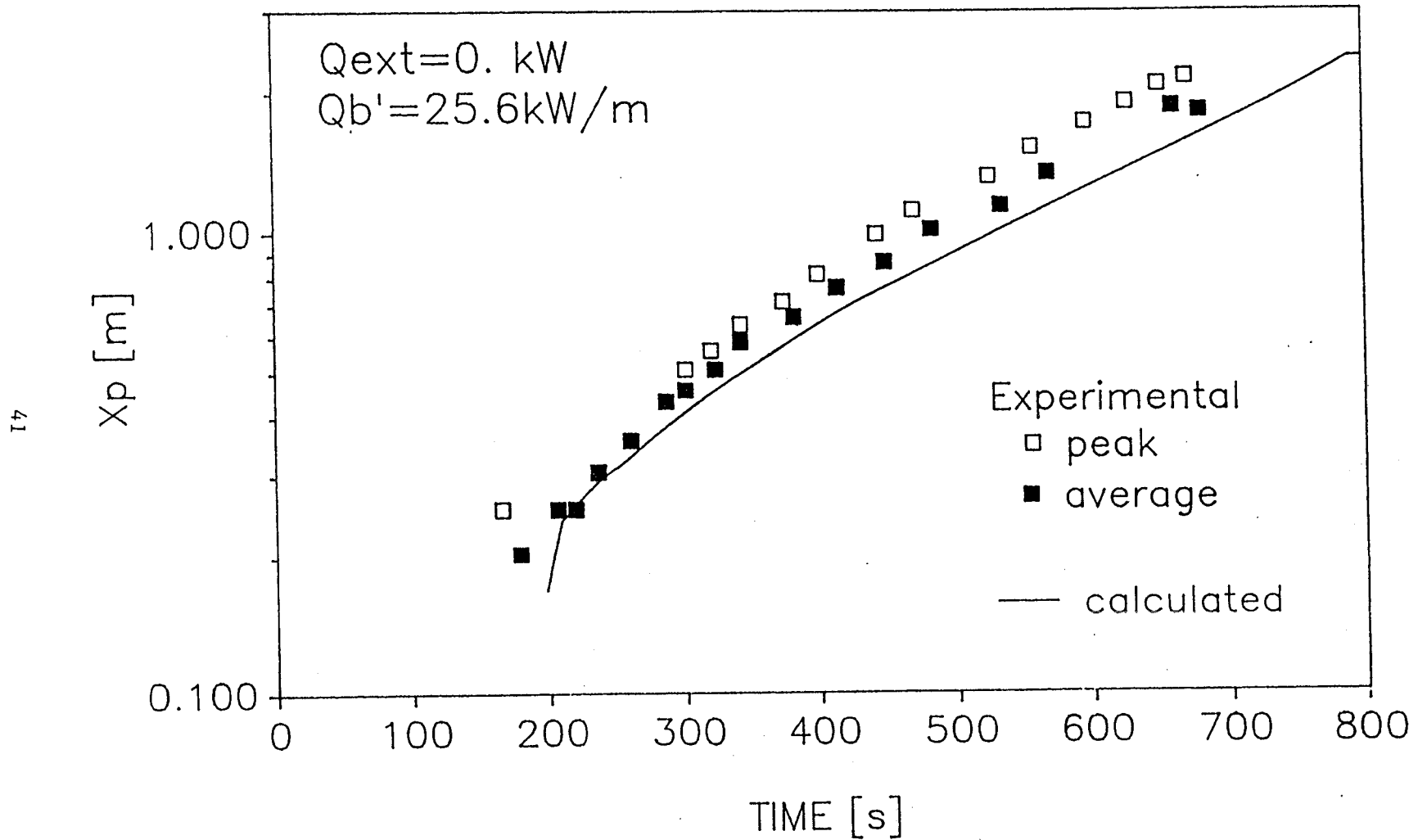


Figure 11. Position of the upper pyrolysis front as a function of time, for thermally-thick PMMA; NIST experiment. The difference between peak and average values arises because the pyrolysis front is not horizontal (three-dimensional burning). The solid curve is calculated.

Figure 12. Input data for calculation with particle board.

See Appendix A for the meaning of the various entries. The files are in the order: material data; burner output and width. In the second row, Cone Calorimeter output; wall temperatures and (external) fluxes.

2.43		0.0000						
0.			2					
670.		0.0000		7.6800				
0.013		600.00		7.6800				
1822.		0.2500						
0.204		0.3000						
668.								
298.								
298.								
2.								
2.								
600.								
1340.								
1.4E7								
0.94								
0.3								
0.927								
12.78								
298.								
298.								
453.								
2.5								
2.5								
0.3								
	15							
	0.000	0.000						
	5.000	25.00						
	10.00	180.0						
	20.00	220.0						
	25.00	220.0	1.0					
	150.0	140.0	0.0	298.0	298.0	0.	0.	
	225.0	120.0						
	325.0	120.0						
	380.0	125.0						
	525.0	240.0						
	565.0	260.0						
	585.0	250.0						
	630.0	100.0						
	675.0	40.00						
	900.0	40.00						
	43220.							

UPWARD FLAMESPREAD
CFR Particle Board

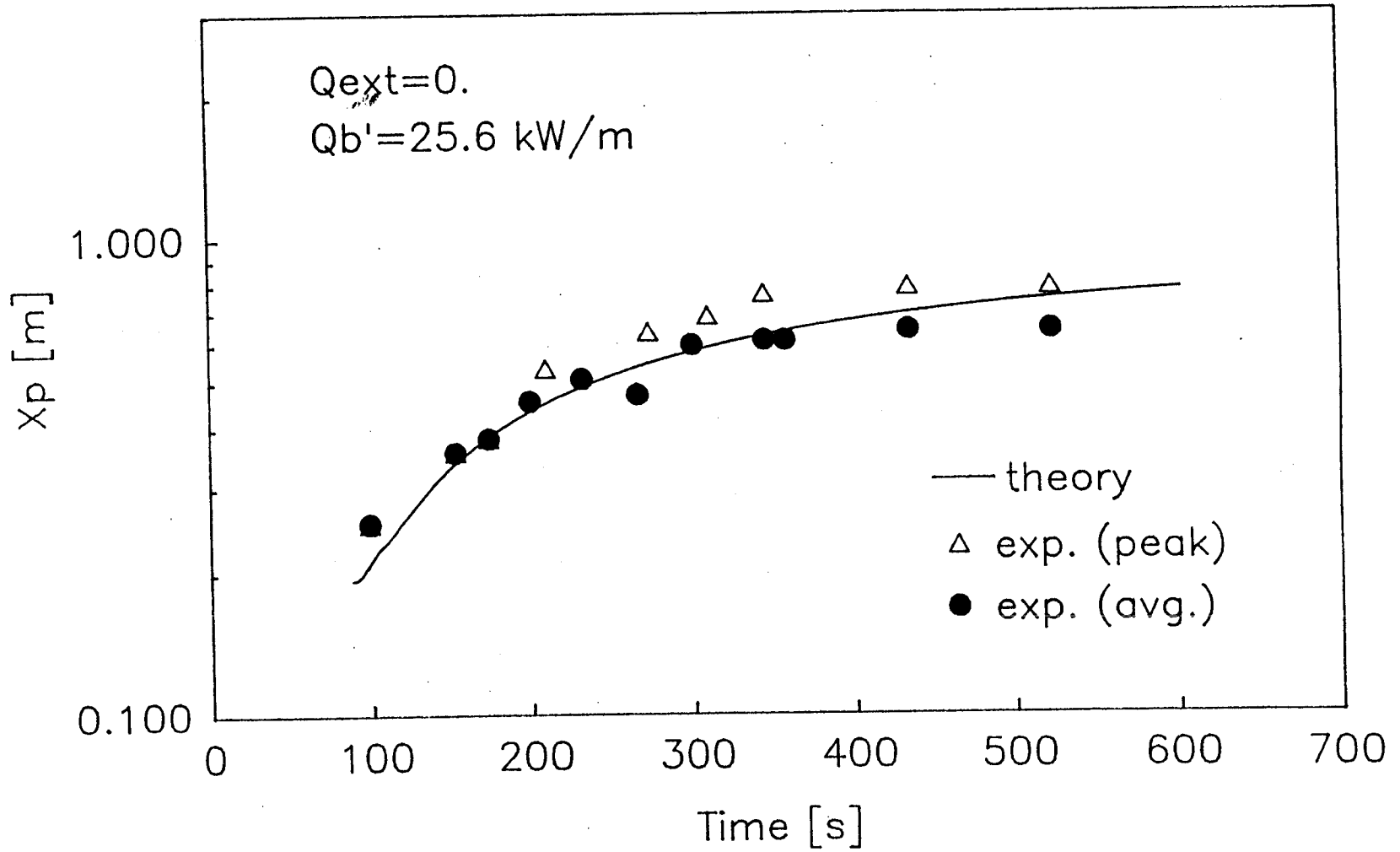


Figure 13. Position of the upper pyrolysis front as a function of time, for particle board. Same remarks as for Fig.11.

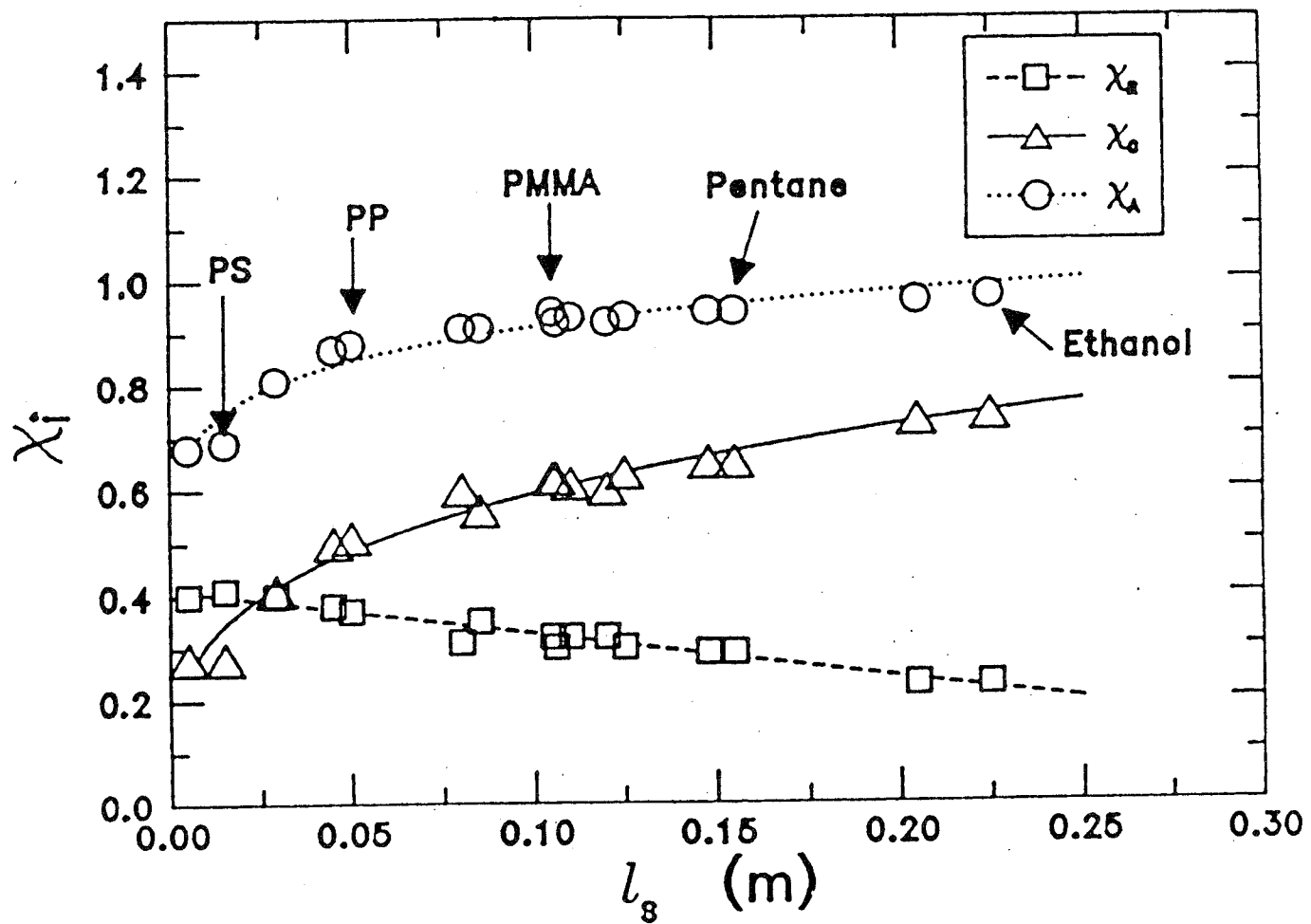


Figure 14. χ_A , χ_C , and χ_R , correlated against the smoke-point height. (Note: $\chi_C \equiv \chi_A - \chi_R$).

Appendix A. Sample list of input for PMMA

Wall Slab Thermophysical Data, Time Step, Etc.

(Input via subroutine FIDAT or KBDAT)

Length of wall/slab (m):	2.43
Height of bottom of slab above floor (m):	0.00
Slab density (kg/m ³):	1180.
Slab thickness (m):	0.0127
Slab specific heat (J/kg-C):	2250.
Thermal conductivity of slab material (W/m-C):	0.311
Ignition temperature (K):	630.
Initial (uniform) temperature of slab (K):	298.
Ambient temperature (K):	298.
Duration of internal time step (s):	2.
Time interval for output (s):	2.
Duration of test (s):	300.
Specific heat of product gases (J/kg-C):	1340.
(Lower) heat of combustion (J/kg):	2.52 E7
Efficiency of combustion:	0.94
Fraction of energy produced in complete combustion that goes into radiation:	0.3
Absorptivity/emissivity of slab:	0.927
Flame spread parameter Φ (kW ² /m ³):	12.78
Temperature of upper wall:	298.
Temperature of lower wall:	298.
Critical temperature for spread (K):	453.
Height of layer interface at current time step (m):	1.22
Layer height at previous time step (m):	1.22
Width of slab (m):	0.31

Sample list of input for PMMA (cont'd)

Cone Calorimeter Data

(Input via subroutine FIMLR or KBMLR)

Number of sets of data points: 12

Time (sec)	Heat Release Rate (kW/m**2)
0.0	0.0
21.	268.
253.	319.
453.	368.
653.	405.
853.	440.
1053.	481.
1253.	556.
1333.	611.
1363.	836.
1407.	366.
1833.	0.

Cone heat flux (W/m²): 21610.

(N.B.: remember the comment made in Section 9, to the effect that **this** is the effective radiation flux when the nominal value is 25 kW/m²).

Burner (Ignitor) Data

(Input via subroutine FIBRN or KBBRN)

Height of burner above floor (m): 0.0

Number of burner data points: 2

Point 1 Time (s): 0.0 Power (kW): 7.68

Point 2 Time (s): 1000.0 Power (kW): 7.68

Fraction of energy produced in complete combustion that goes into radiation

(χ_R): 0.3

Slab width (m): 0.31

Wall Temperature and External Flux Data

(Input via subroutine FIWTMP or KBWTMP)

Number of points at which wall temperature/external flux will be given : 1

Point 1

Time (s): 0.0

Temperature of upper wall (K): 298.

Temperature of lower wall (K): 298.

External flux on upper wall (W/m²): 0.

External flux on lower wall (W/m²): 0.

Appendix B. List of subroutines and function subprograms

Note: the rubric LIB, used below, means "library routine." The symbols used to denote variables, in the explanatory comments below, are those used in the FORTRAN computer code SPREAD.

ROUTINE: BRNFLX

CALLED BY: NETFLX (before ignition); by FLXTMP, MLRATE, and SPRED0 (afterwards)

Calculates the net wall flux for all the nodes at and above $z_s \equiv ZS$: takes the incoming flux and subtracts the reradiated flux from it.

ROUTINE: BRNOUT

LIB: ABS

CALLED BY: SPRED0

Determines whether burnout has occurred at a node (usually, low nodes), and, if so, raises the lower bound (front) of the pyrolysis zone.

ROUTINE: COMBND

CALLED BY: FLXTMP MLRATE SPRED0

Calculates the combined flux to the wall: radiative (flame + external) plus convective.

ROUTINE: COMBST

CALLED BY: MLRATE

Calculates power output from the wall, given the mass-loss rate.

ROUTINE: CVCCOM

CALLS: CVFLX DLTCLC

LIB: EXP

CALLED BY: FLXTMP MLRATE SPRED0

Calculates the convective flux to the wall.

ROUTINE: CVFLX

LIB: EXP

CALLED BY: CVCCOM INFLX

Calculates the convective flux at the height XHGHT.

ROUTINE: DLTCLC

LIB: EXP LOG

CALLED BY: CVCCOM

Calculates delta phi sub c (DLTPHC), the jump in convective heat transfer flux (mostly) below the pyrolysis front.

ROUTINE: FIBRN
CALLED BY: GETDAT

Reads the burner data from a file.

ROUTINE: FIDAT
LIB: MOD
CALLED BY: GETDAT

Reads data from a file named by the user.

ROUTINE: FIMLR
CALLED BY: GETDAT

Reads heat-release rate data from a file and converts it to mass-loss rate data.

ROUTINE: FIWTMP
CALLED BY: GETDAT

Reads the wall temperature and external flux at various times from a file.

ROUTINE: FLAME
LIB: SQRT
CALLED BY: IGNITE MLRATE SPRED0

Calculates flame height.

ROUTINE: FLLTMP
CALLED BY: SETUP

Initializes the arrays used in the program.

ROUTINE: FLXTMP
CALLS: BRNFLX COMBND CVCCOM RADCOM WALTMP
LIB: INT MAX
CALLED BY: SPRED0

Calculates fluxes and temperatures at TIME+DT.

ROUTINE: GETDAT
CALLS: FIBRN FIDAT FIMLR FIWTMP KBBRN KBDAT KBMLR KBWTMP
CALLED BY: SPREAD

Obtains data for the wall fire spread routine.

ROUTINE: IGNCHK
CALLS: SORT WALTMP
CALLED BY: IGNITE

Obtains temperatures at all nodes, checks for ignition at each.

ROUTINE: IGNITE

CALLS: FLAME IGNCHK NETFLX PHIEXL PHIEXU POWOUT TRNSFR WALTMP
LIB: INT
CALLED BY: SPRED

Checks for ignition and calculates the limits of the pyrolysis zone.

ROUTINE: INFLX

CALLS: CVFLX
CALLED BY: NETFLX

Calculates the incoming flux at and above $z_s \equiv ZS$; valid only for nodes below XF (the node closest to x_f).

ROUTINE: INFLXF

CALLED BY: NETFLX

Calculates incoming flux at nodes above XF using PHIF.

ROUTINE: INIMLR

CALLS: TMLRP
CALLED BY: SPRED

Initializes the mass-loss rate, upon ignition.

ROUTINE: KBBRN

CALLED BY: GETDAT

Prompts the user to enter the burner data from the keyboard. The data are then saved in a file.

ROUTINE: KBDAT

LIB: MOD
CALLED BY: GETDAT

Enters data from the keyboard. It will save the data in a file which may be used later with the option to read that data from a file.

ROUTINE: KBMLR

CALLED BY: GETDAT

Prompts the user to enter heat-release rate data from the keyboard. The data are then saved in a file. The heat-release rates are converted to mass-loss rates for internal use by the program.

ROUTINE: KBWTMP

CALLED BY: GETDAT

Prompts the user to enter the wall temperature and external flux at various times from the keyboard. The data are then saved in a file.

ROUTINE: LATSPR
CALLED BY: SPRED0

Calculates the lateral spread.

ROUTINE: MLRATE
CALLS: BRNFLX COMBND COMBST CVCCOM FLAME NBFLUX RADCOM TMLRP
LIB: INT MAX MOD
CALLED BY: SPRED0

Calculates the mass-loss rate at TIME+DT, using Cone calorimeter data.

ROUTINE: NBFLUX
CALLED BY: MLRATE NETFLX

Calculates the incoming flux when there is no burner.

ROUTINE: NETFLX
CALLS: BRNFLX INFLX INFLXF NBFLUX RADIAT
CALLED BY: IGNITE

Calculates net flux: incoming minus reradiative, before ignition.

ROUTINE: PHIEXL
CALLED BY: IGNITE SPRED0

Performs an interpolation on a set of data obtaining the EXTERNAL FLUX (for lower layer) at a specific time.

ROUTINE: PHIEXU
CALLED BY: IGNITE SPRED0

Performs an interpolation on a set of data obtaining the EXTERNAL FLUX (for upper layer) at a specific time.

ROUTINE: POWOUT
CALLED BY: IGNITE SPRED0

Performs an interpolation on a set of data obtaining the power output for the burner at a specific time.

ROUTINE: RADCOM
LIB: EXP MAX
CALLED BY: FLXTMP MLRATE

Calculates the combined radiation flux (burner + wall).

ROUTINE: RADIAT

CALLS: RDFLX
CALLED BY: NETFLX

Calculates the radiative flux (from the burner flame alone).

ROUTINE: RDFLX

LIB: EXP
CALLED BY: RADIAT

Calculates the radiative flux from a burner.

ROUTINE: SETUP

CALLS: FLLTMP
LIB: ATAN INT MIN SQRT
CALLED BY: SPRED

Initializes variables for IGNITE, INIMLR, and SPREDO.

ROUTINE: SORT

CALLED BY: IGNCHK

Sorts integer array IGNITD(1) to IGNITD(ICOUNT) in ascending order.

ROUTINE: SPREAD

CALLS: GETDAT SPRED
CALLED BY: NONE; i.e., NO ROUTINES CALL SPREAD

Drives the wall fire spread routine SPRED.

ROUTINE: SPRED

CALLS: IGNITE INIMLR SETUP SPREDO
CALLED BY: SPREAD

Drives the spread routines. It calls subroutines to initialize variables, check for ignition, initialize the mass-loss rate, and calculate the spread rate.

ROUTINE: SPREDO

CALLS: BRNFLX BRNOUT COMBND CVCCOM FLAME FLXTMP LATSPR
MLRATE PHIEXL PHIEXU POWOUT UPNDWN WTLO WTUP
LIB: MOD
CALLED BY: SPRED

Main time-step loop for calculating spread.

ROUTINE: SPRED2

CALLS: XTWRD2 XTWRML
CALLED BY: UPNDWN

Tests for spread above or below the pyrolysis front.

ROUTINE: TMLRP

CALLS: TMLRP
LIB: MAX
CALLED BY: INIMLR MLRATE TMLRP

Calculates the total mass loss rate per unit width.

ROUTINE: TMPW04

CALLED BY: WALTMP

Calculates the temperature profile within slab using a discrete grid. The wall is heated or cooled on each side by fluxes and the heat diffuses through it by conduction. The heat diffusion is calculated using an explicit method. Slab geometry (one-dimensional heat flow) is assumed.

ROUTINE: TRNSFR

CALLED BY: IGNITE

Transfers current temperature array to array TEMP1.

ROUTINE: UPNDWN

CALLS: SPRED2
LIB: INT
CALLED BY: SPRED0

Checks for upward and downward spread.

ROUTINE: WALTMP

CALLS: TMPW04
CALLED BY: FLXTMP IGNCHK IGNITE

Finds the temperature profile at each node. The array TEMP1(i,j), where i corresponds to the ith node, and j to the depth y_j , contains all the temperatures; the element TEMP1(i,1) is the surface temperature at node i.

ROUTINE: WTLO

CALLED BY: SPRED0

Performs an interpolation on a set of data obtaining the lower wall surface temperature at a specific time.

ROUTINE: WTUP
CALLED BY: SPRED0

Performs an interpolation on a set of data obtaining the upper wall surface temperature at a specific time.

ROUTINE: XTWRD2
CALLED BY: SPRED2

Calculates next XP or XPB of the pyrolysis zone if spread occurred when highest or lowest pyrolyzing node is higher than M or lower than L-1.

ROUTINE: XTWRML
CALLED BY: SPRED2

Calculates next XP or XPB of the pyrolysis zone if spread occurred when highest or lowest pyrolyzing node is M or L-1.

*** LIBRARY ROUTINES ***

ROUTINE: ABS
CALLED BY: BRNOUT

ROUTINE: ATAN
CALLED BY: SETUP

ROUTINE: EXP
CALLED BY: CVCCOM CVFLX DLTCLC RADCOM RDFLX

ROUTINE: INT
CALLED BY: FLXTMP IGNITE MLRATE SETUP UPNDWN

ROUTINE: LOG
CALLED BY: DLTCLC

ROUTINE: MAX
CALLED BY: FLXTMP MLRATE RADCOM TMLRP

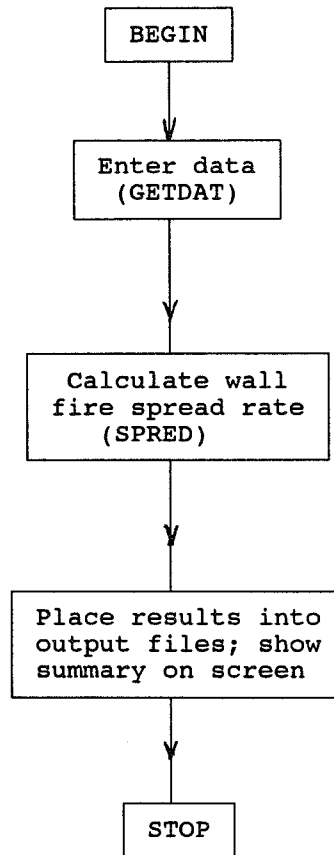
ROUTINE: MIN
CALLED BY: SETUP

ROUTINE: MOD
CALLED BY: FIDAT KBDAT MLRATE SPRED0

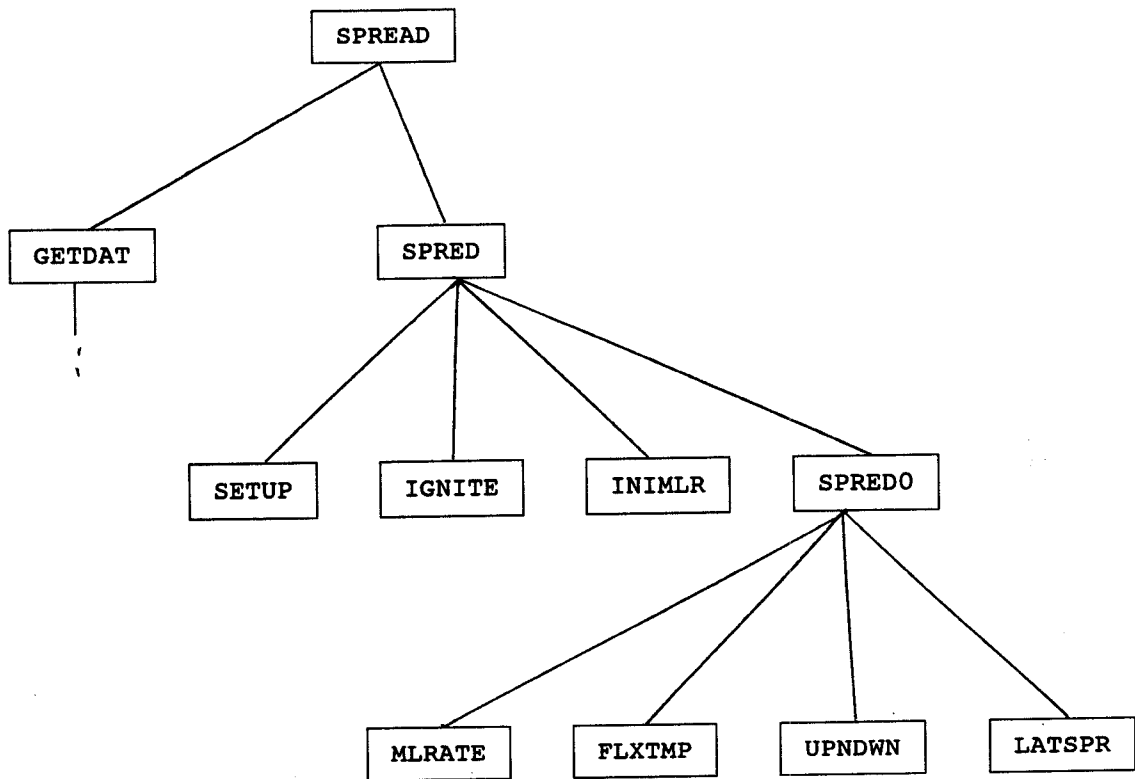
ROUTINE: SORT
CALLED BY: FLAME SETUP

Appendix C: Structure of SPREAD, via block/flow diagrams.

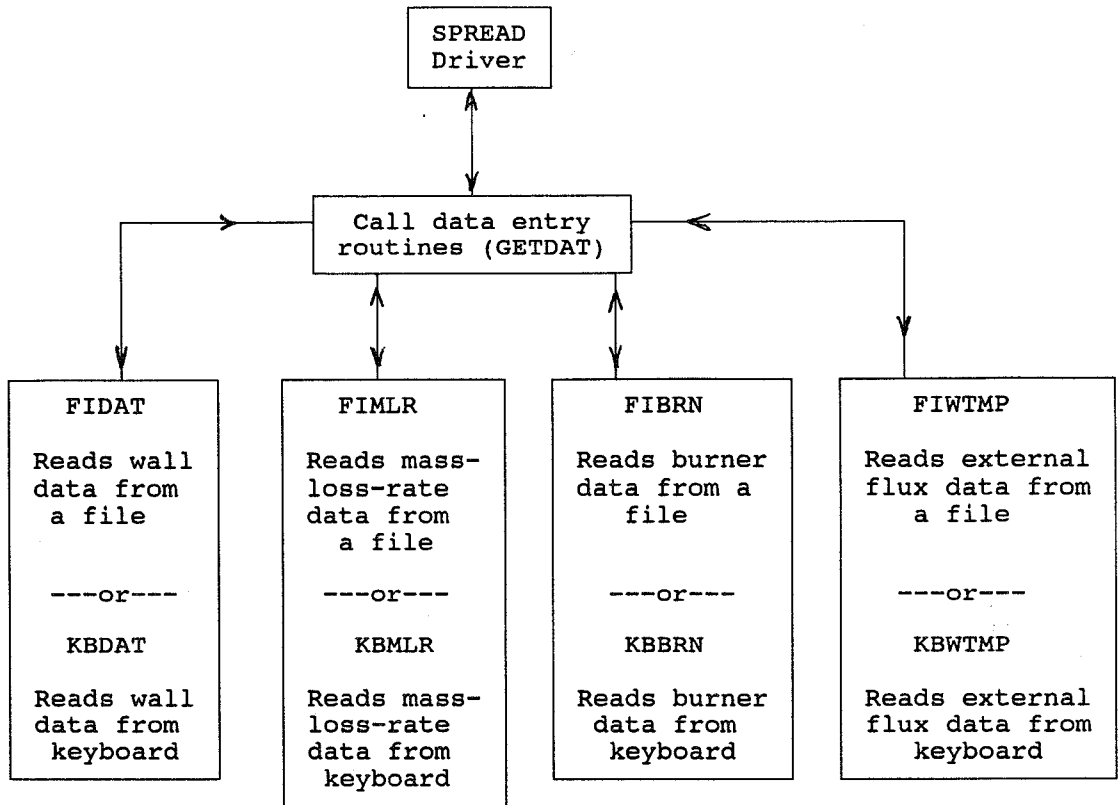
C1. Overview of program (note: subroutines which implement a particular procedure are shown in parentheses)



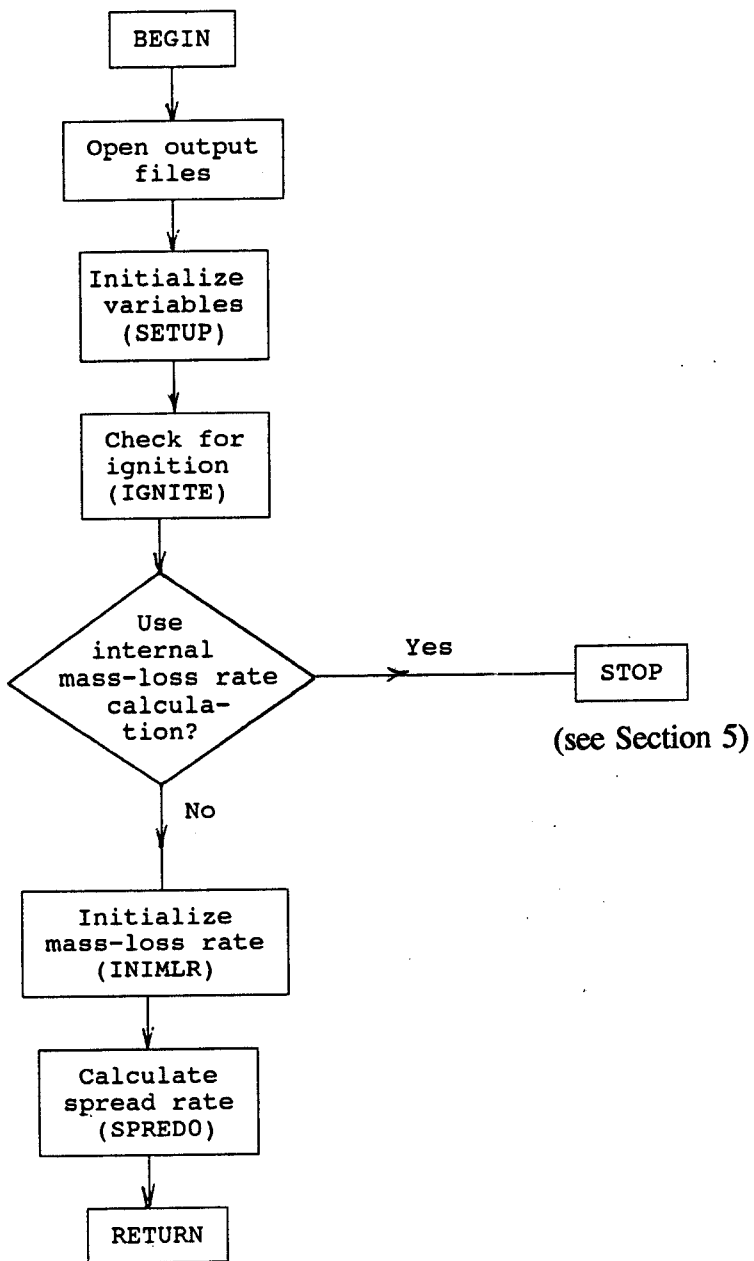
C2. Somewhat more detailed structure map



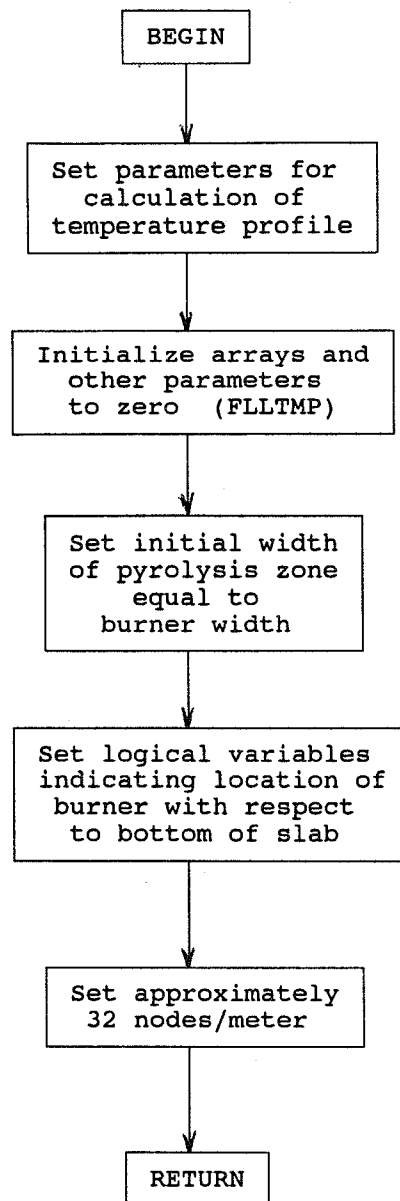
C3. Subroutine GETDAT



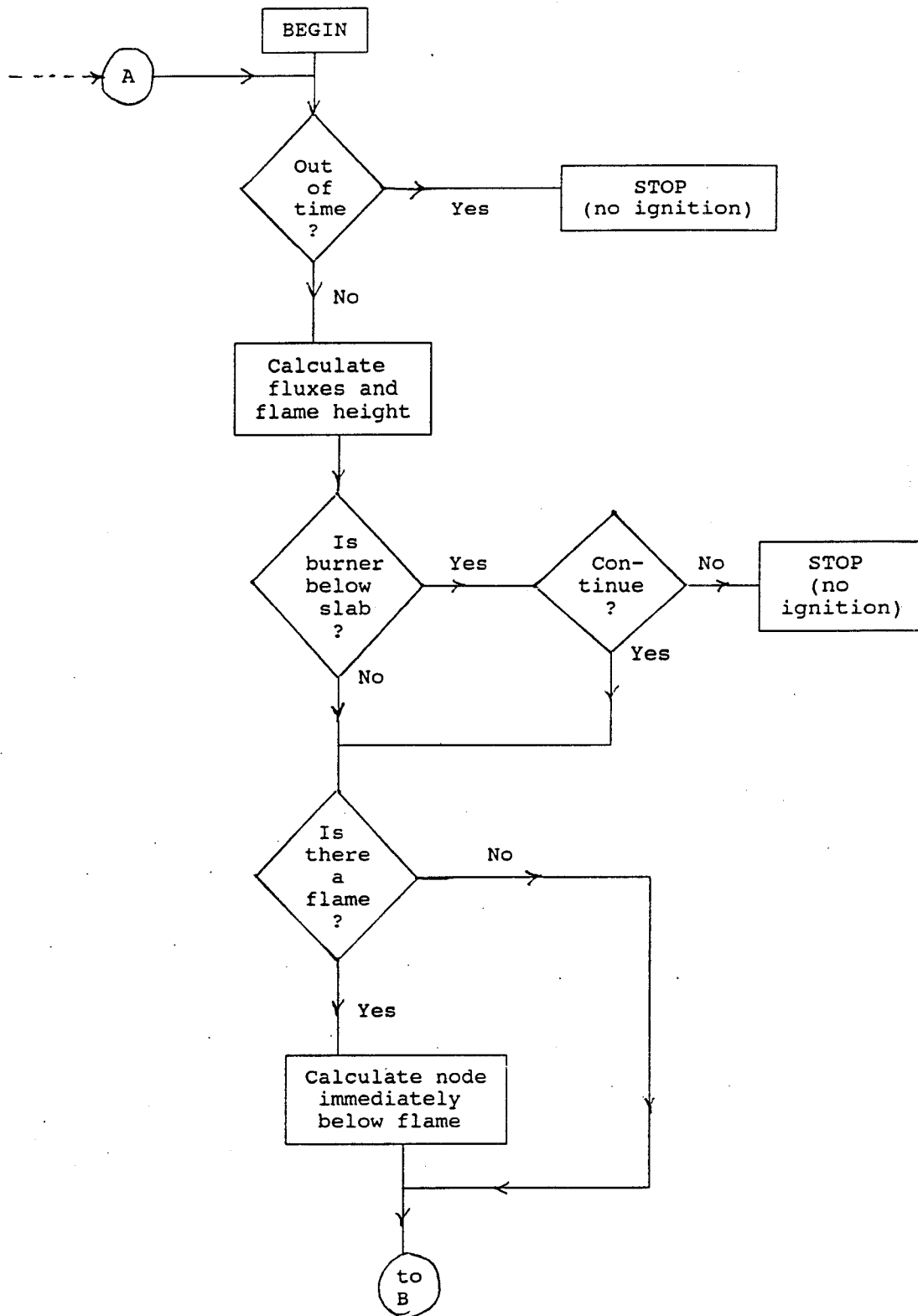
C4. Structure of subroutine SPRED (the main calculation)



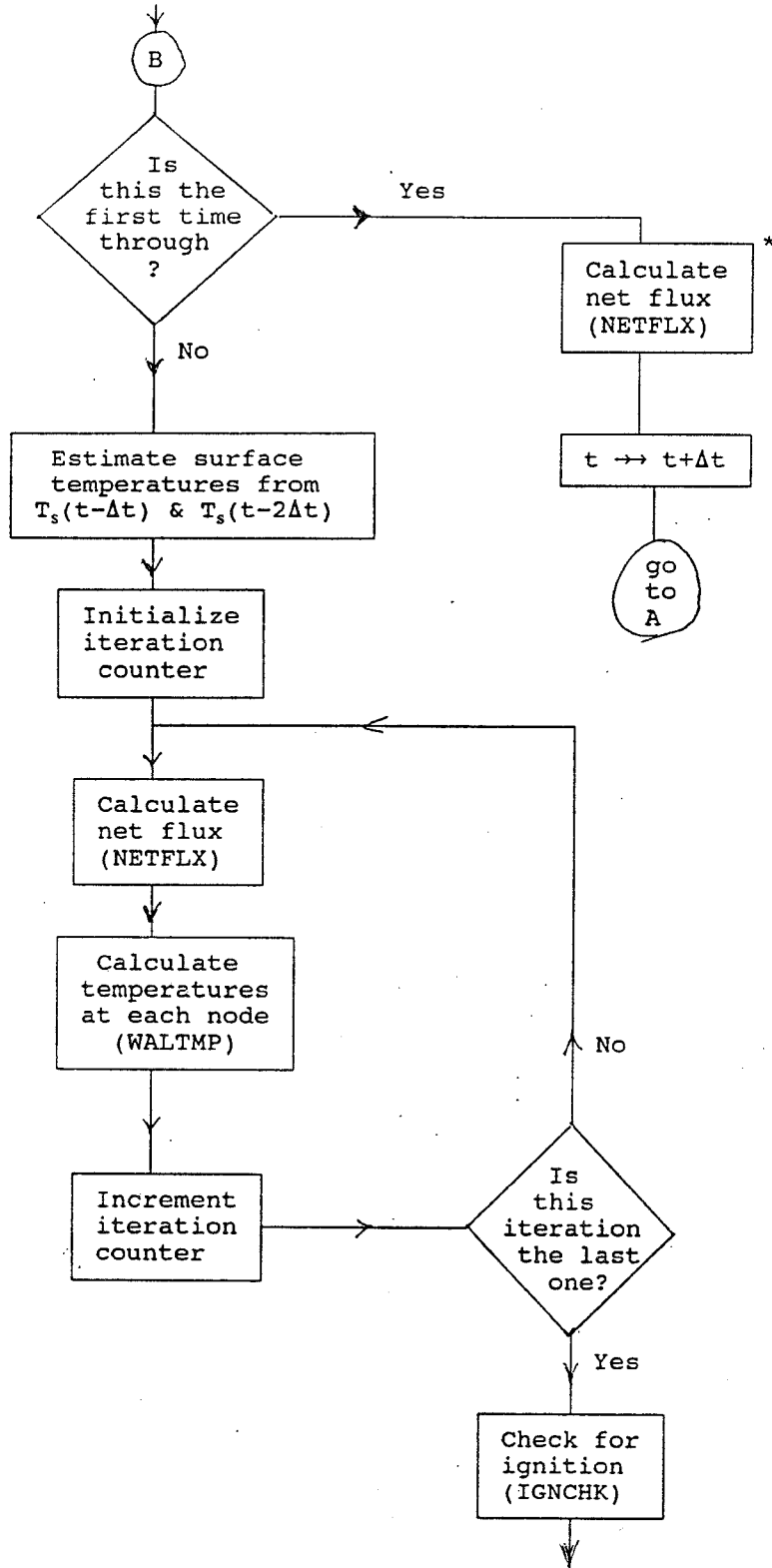
C5. Subroutine SETUP



C6. Subroutine IGNITE

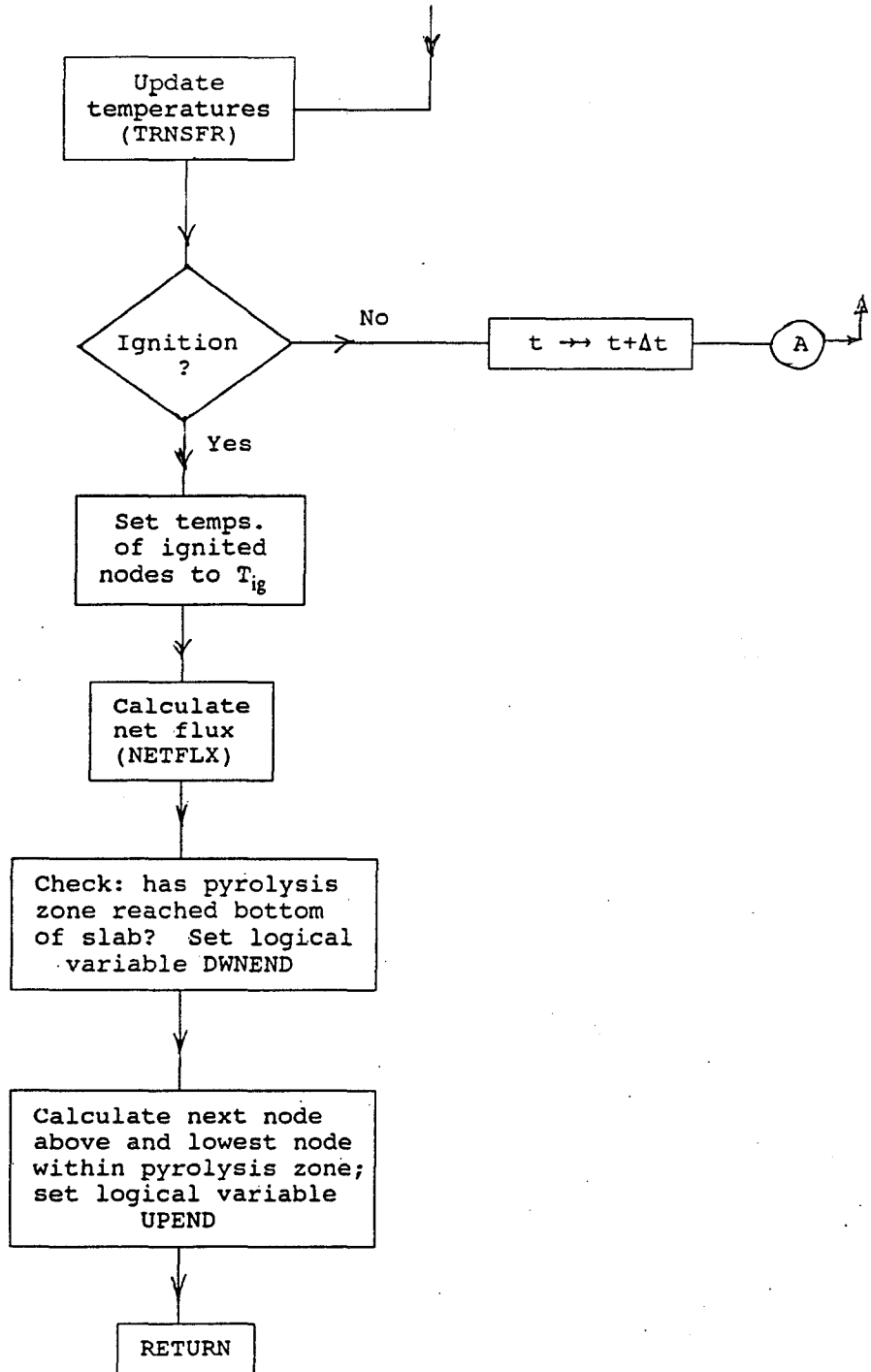


Subroutine IGNITE (continued)

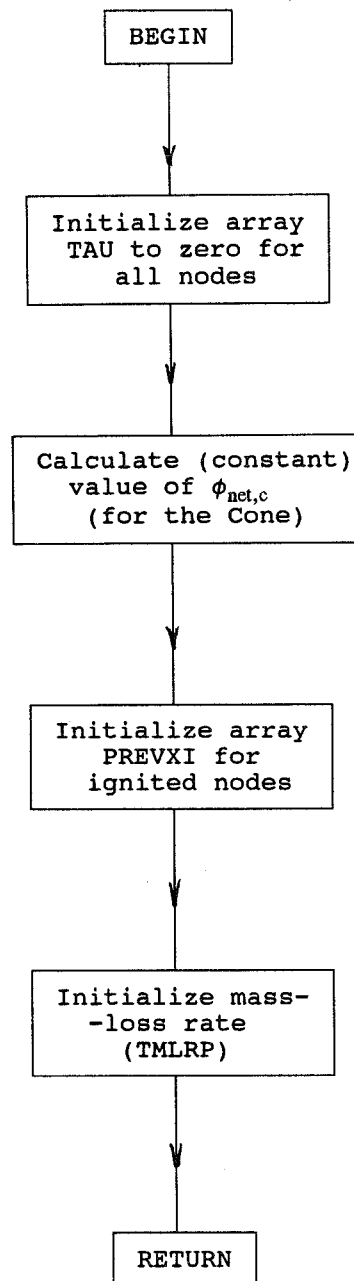


* Flux is needed at both beginning and end of a time interval in order to make the wall temperature calculation

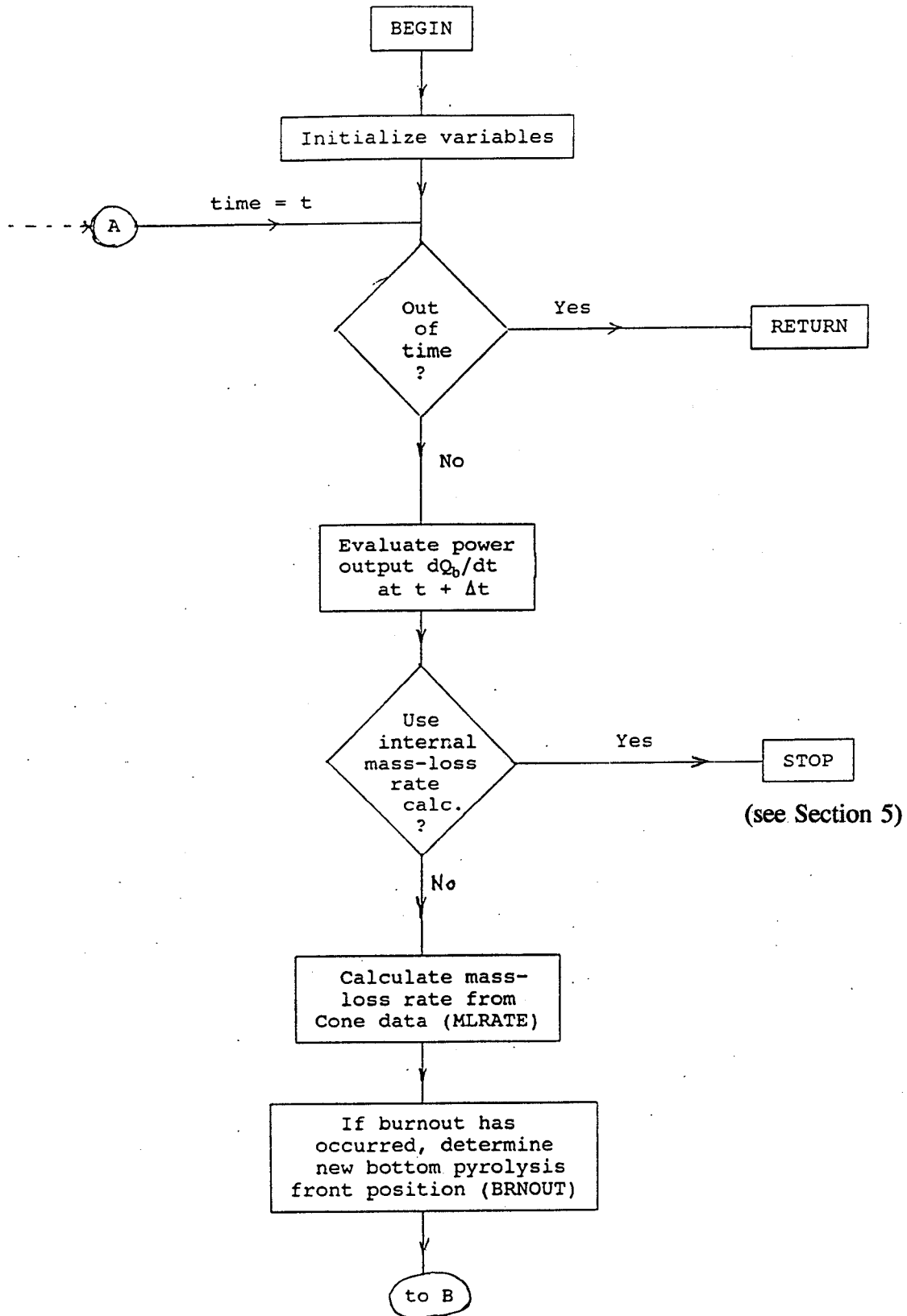
Subroutine IGNITE (continued)



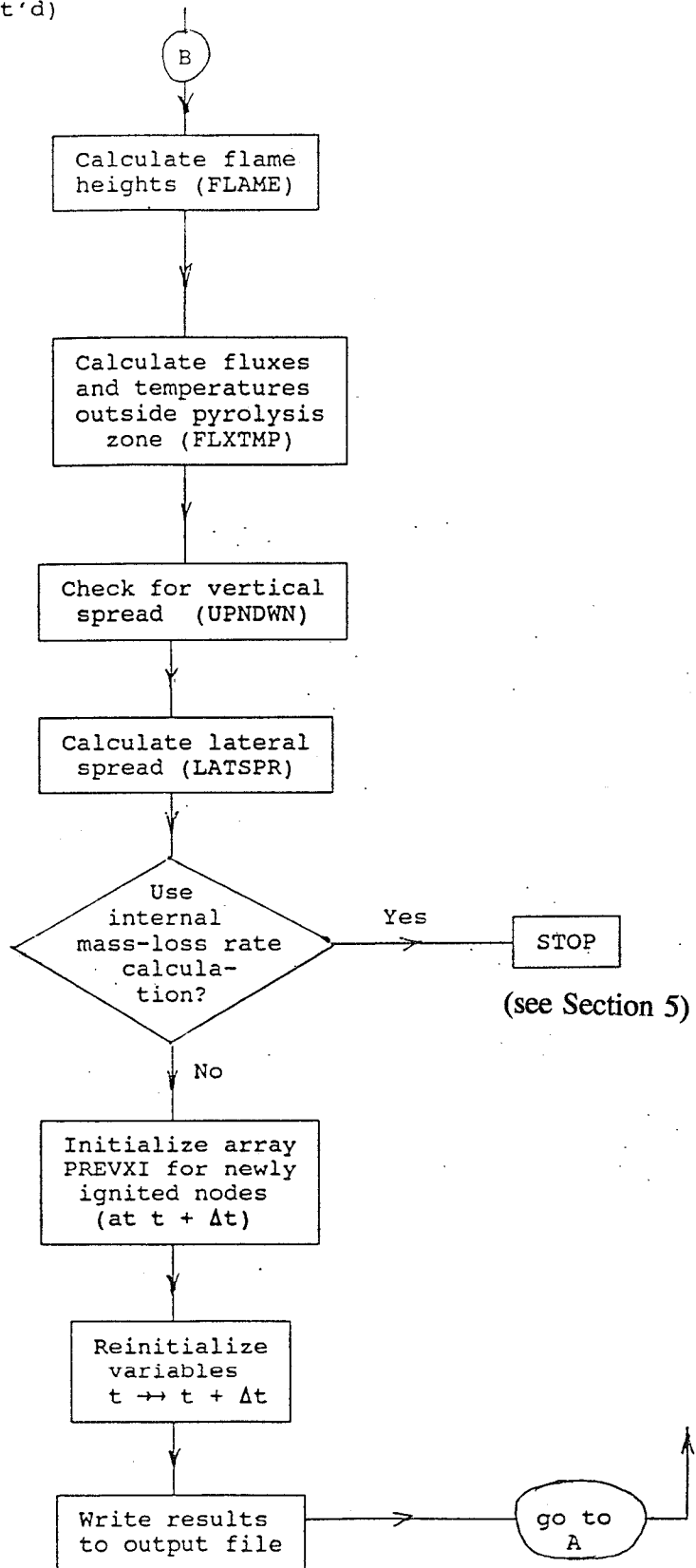
C7. Subroutine INIMLR



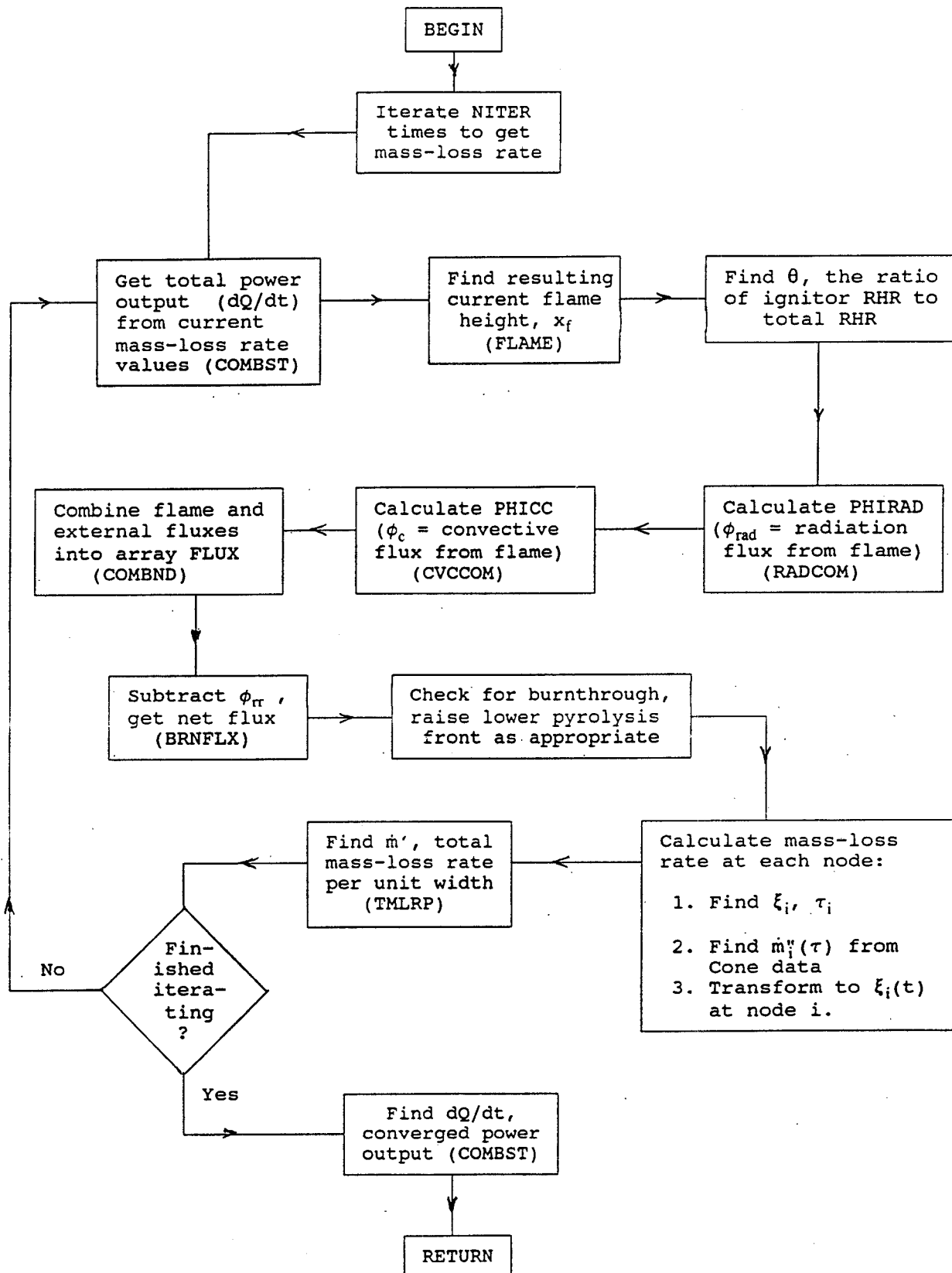
C8. Subroutine SPREADO



Subroutine SPREDO (cont'd)



C9. Subroutine MLRATE



NIST-114 (REV. 9-92) ADMAN 4.09	U.S. DEPARTMENT OF COMMERCE NATIONAL INSTITUTE OF STANDARDS AND TECHNOLOGY	(ERB USE ONLY) <table border="1" style="width:100%; border-collapse: collapse;"> <tr> <td style="width:50%;">ERB CONTROL NUMBER</td> <td style="width:50%;">DIVISION</td> </tr> <tr> <td>PUBLICATION REPORT NUMBER</td> <td>CATEGORY CODE</td> </tr> <tr> <td style="text-align: center;">NISTIR 5619</td> <td></td> </tr> <tr> <td>PUBLICATION DATE</td> <td>NUMBER PRINTED PAGES</td> </tr> <tr> <td style="text-align: center;">February 1995</td> <td></td> </tr> </table>	ERB CONTROL NUMBER	DIVISION	PUBLICATION REPORT NUMBER	CATEGORY CODE	NISTIR 5619		PUBLICATION DATE	NUMBER PRINTED PAGES	February 1995	
ERB CONTROL NUMBER	DIVISION											
PUBLICATION REPORT NUMBER	CATEGORY CODE											
NISTIR 5619												
PUBLICATION DATE	NUMBER PRINTED PAGES											
February 1995												
MANUSCRIPT REVIEW AND APPROVAL												

INSTRUCTIONS: ATTACH ORIGINAL OF THIS FORM TO ONE (1) COPY OF MANUSCRIPT AND SEND TO:
 THE SECRETARY, APPROPRIATE EDITORIAL REVIEW BOARD.

TITLE AND SUBTITLE (CITE IN FULL)
 SPREAD - A Model of Flame Spread on Vertical Surfaces

CONTRACT OR GRANT NUMBER	TYPE OF REPORT AND/OR PERIOD COVERED February 1993
--------------------------	---

AUTHOR(S) (LAST NAME, FIRST INITIAL, SECOND INITIAL) Mitler, H.E. and Steckler, K.D.	PERFORMING ORGANIZATION (CHECK (X) ONE BOX) <input checked="" type="checkbox"/> NIST/GAITHERSBURG <input type="checkbox"/> NIST/BOULDER <input type="checkbox"/> JILA/BOULDER
---	--

LABORATORY AND DIVISION NAMES (FIRST NIST AUTHOR ONLY)
 Building and Fire Research Laboratory/Fire Safety Engineering Division

SPONSORING ORGANIZATION NAME AND COMPLETE ADDRESS (STREET, CITY, STATE, ZIP)

RECOMMENDED FOR NIST PUBLICATION

<input type="checkbox"/> JOURNAL OF RESEARCH (NIST JRES)	<input type="checkbox"/> MONOGRAPH (NIST MN)	<input type="checkbox"/> LETTER CIRCULAR
<input type="checkbox"/> J. PHYS. & CHEM. REF. DATA (JPCRD)	<input type="checkbox"/> NATL. STD. REF. DATA SERIES (NIST NSRDS)	<input type="checkbox"/> BUILDING SCIENCE SERIES
<input type="checkbox"/> HANDBOOK (NIST HB)	<input type="checkbox"/> FEDERAL INF. PROCESS. STDS. (NIST FIPS)	<input type="checkbox"/> PRODUCT STANDARDS
<input type="checkbox"/> SPECIAL PUBLICATION (NIST SP)	<input type="checkbox"/> LIST OF PUBLICATIONS (NIST LP)	<input type="checkbox"/> OTHER _____
<input type="checkbox"/> TECHNICAL NOTE (NIST TN)	<input checked="" type="checkbox"/> NIST INTERAGENCY/INTERNAL REPORT (NISTIR)	

RECOMMENDED FOR NON-NIST PUBLICATION (CITE FULLY)	<input type="checkbox"/> U.S.	<input type="checkbox"/> FOREIGN	PUBLISHING MEDIUM
			<input checked="" type="checkbox"/> PAPER <input type="checkbox"/> DISKETTE (SPECIFY) _____ <input type="checkbox"/> OTHER (SPECIFY) _____
			<input type="checkbox"/> CD-ROM

SUPPLEMENTARY NOTES

ABSTRACT (A 2000-CHARACTER OR LESS FACTUAL SUMMARY OF MOST SIGNIFICANT INFORMATION. IF DOCUMENT INCLUDES A SIGNIFICANT BIBLIOGRAPHY OR LITERATURE SURVEY, CITE IT HERE. SPELL OUT ACRONYMS ON FIRST REFERENCE.) (CONTINUE ON SEPARATE PAGE, IF NECESSARY.)

This report describes the computer program SPREAD. SPREAD is the explicit implementation of a model which has been developed for predicting the ignition of, and the subsequent rate and extent of fire spread on flat walls in a room using the fire properties of the materials involved. It uses input data from bench-scale tests including the LIFT and the Cone Calorimeter. The principal mode of spread is upward, but the calculations also include the slow lateral spread on the wall. For the latter calculations, the fact that the room produces a two-layer environment has been taken into account (the lateral spread rate within the upper layer is greater than in the lower one). Embedded in the overall model is a general pyrolysis submodel, specially developed for this purpose, which treats arbitrary materials (ablating, char-forming, composite, etc.). SPREAD also calculates the regression of the pyrolyzing surface, including the possible burnout of the wall/slab at any point. The program has been compared to experimental data for wood particle board and for PMMA. The structure of the program is given in a set of appendices.

KEY WORDS (MAXIMUM 9 KEY WORDS; 28 CHARACTERS AND SPACES EACH; ALPHABETICAL ORDER; CAPITALIZE ONLY PROPER NAMES)

computer models; fire growth; fire models; fire spread; mathematical models; upward spread; wall fires

AVAILABILITY

<input checked="" type="checkbox"/> UNLIMITED	<input type="checkbox"/> FOR OFFICIAL DISTRIBUTION. DO NOT RELEASE TO NTIS.
<input type="checkbox"/> ORDER FROM SUPERINTENDENT OF DOCUMENTS, U.S. GPO, WASHINGTON, D.C. 20402	
<input checked="" type="checkbox"/> ORDER FROM NTIS, SPRINGFIELD, VA 22161	

NOTE TO AUTHOR(S) IF YOU DO NOT WISH THIS MANUSCRIPT ANNOUNCED BEFORE PUBLICATION, PLEASE CHECK HERE.